Computer Methods in Applied Mechanics and Engineering 432 (2024) 117443

Contents lists available at ScienceDirect

Comput. Methods Appl. Mech. Engrg.

journal homepage: www.elsevier.com/locate/cma

# Optimal control of constrained mechanical systems in redundant coordinates: Formulation and structure-preserving discretization

Simeon Schneider, Peter Betsch *

*Institute of Mechanics, Karlsruhe Institute of Technology, Otto-Ammann-Platz 9, Karlsruhe, 76131, Germany*

ARTICLE INFO

*Keywords:*
Differential–algebraic equations
Structure-preserving discretization
Generalized momentum maps
GGL stabilization
Quadratic invariants

ABSTRACT

This work deals with optimal control problems for constrained mechanical systems whose motion is governed by differential algebraic equations (DAEs). Both index-3 DAEs and stabilized index-2 DAEs are considered. Two alternative formulations of the optimal control problem are compared to each other. It is shown that symmetries of the optimal control problem lead to the conservation of generalized momentum maps. These generalized momentum maps are related to quadratic invariants of the optimal control problem. A direct discretization approach is newly proposed which is (i) capable to conserve the quadratic invariants, and (ii) equivalent to the indirect approach to the optimal control problem. Numerical examples are presented to access the properties of the newly developed schemes.

## 1. Introduction

The present work deals with the optimal control of constrained mechanical systems, whose motion is described by differential–algebraic equations (DAEs). In particular, we focus on mechanical systems subject to scleronomic holonomic constraints. The constraints give rise to redundant coordinates and facilitate the singularity-free description of arbitrarily complex discrete mechanical systems. We concentrate on optimal control problems in which the DAEs play the role of the state equations. This treatment ensures that the mechanical system stays on the correct configuration manifold and thus prevents the numerical drift-off phenomenon. We refer to [1] for a recent account of alternative approaches to the optimal control of constrained mechanical systems.

It is well-known that the motion of holonomically constrained mechanical systems is governed by DAEs with differentiation index three [2,3]. In the context of optimal control problems these DAEs play the role of the state equations. Numerical methods for the optimal control of DAEs are much less mature than those for ODEs [4]. This is particularly true for the index-3 DAEs associated with constrained mechanical systems. Even if the often applied GGL (Gear–Gupta–Leimkuhler [5]) type index reduction is applied, one still has to deal with stabilized index-2 DAEs.

While the modeling of mechanical systems in general requires the imposition of constraints, in some occasions minimal (or local) coordinates might be used. Then the state equations assume the form of ODEs and well-established numerical methods can be applied to solve related optimal control problems, see, for example, [6,7]. Similar observations apply if projection methods are used to eliminate the constraints from the underlying DAEs prior to optimization, see [8–10].

While the Pontryagin maximum principle for the optimal control of ODEs goes back to 1956 [11], a maximum principle for the optimal control of DAEs with index up to three was only published in 2002 [12]. As mentioned in [12], there is common belief that one can apply the standard maximum principle to DAEs as well. The standard procedure relies on the direct use of the holonomic constraints in the optimal control formulation and is used quite often in the field of computational mechanics, see, for

* Corresponding author.
*E-mail address:* peter.betsch@kit.edu (P. Betsch).

https://doi.org/10.1016/j.cma.2024.117443
Received 28 June 2024; Received in revised form 1 October 2024; Accepted 1 October 2024
Available online 11 October 2024

example, [13–15]. The same observation applies to adjoint methods for dynamic optimization problems [16–18]. In contrast to that, the approach complying with the maximum principle [12] has been rarely applied [19,20]. This is particularly true for the high-index DAEs associated with mechanical systems.

Interestingly, to the best of our knowledge, a comparison of the two alternative approaches (common procedure versus maximum principle [12]) to the optimal control of constrained mechanical systems has not been undertaken so far. It is one main goal of this work to fill this gap.

A second main goal of this work is to develop structure-preserving numerical methods for the optimal control of constrained mechanical systems. In the optimal control of ODEs, the conservation of quadratic invariants plays a crucial role, as has been shown by Sanz-Serna [21]. Accordingly, besides the preservation of quadratic invariants, discretization and optimization commute if symplectic (partitioned) Runge–Kutta integration is applied (see also [7,22–24]). Put in other words, if symplectic (partitioned) Runge–Kutta methods are used for the discretization, the direct and indirect approach to the numerical solution of optimal control problems are equivalent. The preservation of quadratic invariants can be linked to Noether's theorem for optimal control [25,26]. In particular, in the optimal control of mechanical systems, generalized momentum maps are conserved if the optimal control problem has symmetry. A corresponding structure-preserving direct method, which is capable to conserve generalized momentum maps of the underlying optimal control problem has been proposed in [27].

In this work we aim to extend the above-mentioned results for the optimal control of ODEs to the realm of constrained mechanical systems whose motion is governed by stabilized index-2 and index-3 DAEs. We show that there exist generalized momentum maps which are (at most quadratic) invariants of the optimal control problem, provided that specific symmetry conditions are fulfilled (see also [28] for a preliminary work). Based on this observation, we aim at structure-preserving numerical methods

- that are capable to preserve generalized momentum maps associated with symmetries of the underlying optimal control problem.
- for which the direct and the indirect approach commute.

These goals shall be addressed in the light of the two alternative optimal control formulations at hand (according to either the common approach or the maximum principle [12]).

The rest of this work is organized as follows. In Section 2, we summarize the equations of motion pertaining to constrained mechanical systems described in terms of redundant coordinates. In addition to the index-3 DAEs we also deal with a GGL type stabilized index-2 variant of the DAEs. The two alternative approaches to the formulation of the optimal control problem are addressed in Section 3. The conservation properties of the optimal control problem are investigated in Section 4. Structure-preserving approaches to the discretization of the optimal control problem are developed in Section 5. The numerical results presented in Section 6 give rise to the reconciliation of the two alternative optimal control formulations in Section 7. Eventually, conclusions are drawn in Section 8.

## 2. The state equations for constrained mechanical systems

In the present work we deal with mechanical systems subject to holonomic constraints. Let $\mathcal{M}$ be a smooth manifold of dimension $n$ and $\mathbf{q} \in \mathcal{M}$ the representation of the local coordinates on $\mathcal{M}$. Due to the presence of constraints the coordinates are redundant. Consequently, the configuration space of the mechanical system is defined by

$$\mathcal{Q} := \{\mathbf{q} \in \mathcal{M} \mid \mathbf{g}^q(\mathbf{q}) = \mathbf{0}\} \tag{1}$$

The constraint function $\mathbf{g}^q(\mathbf{q}) : \mathcal{M} \to \mathbb{R}^m$ defines $m$ independent constraints so that the constraint Jacobian $D\mathbf{g}^q(\mathbf{q})$ has full rank. Correspondingly, the mechanical system has $n_{\text{dof}} = n - m$ degrees of freedom. Differentiating the constraints with respect to time yields the consistency condition $d\mathbf{g}^q(\mathbf{q})/dt = D\mathbf{g}^q(\mathbf{q})\dot{\mathbf{q}} = \mathbf{0}$, where $\dot{\mathbf{q}} \in \mathcal{T}_q\mathcal{Q}$ denotes the velocity vector. Introducing the conjugate momentum $\mathbf{p} = \mathbf{M}\dot{\mathbf{q}}$, the constraints on velocity level can be rewritten as

$$\mathbf{g}^v(\mathbf{q}, \mathbf{p}) = D\mathbf{g}^q(\mathbf{q})\mathbf{M}^{-1}\mathbf{p} = \mathbf{0} \tag{2}$$

Here, $\mathbf{M} \in \mathbb{R}^{n\times n}$ is the symmetric, positive definite mass matrix which is assumed to be constant for simplicity. For later use we introduce matrix

$$\mathbf{A}(\mathbf{q}) = D\mathbf{g}^q(\mathbf{q})\mathbf{M}^{-1}D\mathbf{g}^q(\mathbf{q})^T \tag{3}$$

which is symmetric and non-singular due to the full-rank of the constraint Jacobian $D\mathbf{g}^q(\mathbf{q})$ and the positive definiteness of mass matrix $\mathbf{M}$. The phase space corresponding to the configuration manifold (1) can be introduced as

$$\mathcal{T}^*\mathcal{Q} := \{(\mathbf{q}, \mathbf{p}) \in \mathcal{T}^*\mathcal{M} \mid \mathbf{g}^q(\mathbf{q}) = \mathbf{0}, \mathbf{g}^v(\mathbf{q}, \mathbf{p}) = \mathbf{0}\} \tag{4}$$

Accordingly, the phase space $\mathcal{T}^*\mathcal{Q}$ has dimension $2n_{\text{dof}}$. Note that the constraints on velocity level (2) are also referred to as hidden constraints.

### 2.1. The state equations as index-3 DAEs

To describe the motion of the mechanical system we introduce the augmented mechanical Hamiltonian

$$H_3^M(\mathbf{q}, \mathbf{p}, \mathbf{y}_q) = T(\mathbf{q}, \mathbf{p}) + V(\mathbf{q}) + \mathbf{y}_q^T\mathbf{g}^q(\mathbf{q}) \tag{5}$$

where $T : \mathcal{T}^*\mathcal{M} \to \mathbb{R}$ is the kinetic energy defined by

$$T(\mathbf{q}, \mathbf{p}) = \frac{1}{2}\mathbf{p}^T\mathbf{M}^{-1}\mathbf{p} \tag{6}$$

$V : \mathcal{M} \to \mathbb{R}$ is the potential energy and $\mathbf{y}_q \in \mathbb{R}^m$ are Lagrangian multipliers associated with the constraints. The motion of the constrained Hamiltonian system is governed by the differential–algebraic equations (DAEs)

$$\dot{\mathbf{q}} = \quad \nabla_{\mathbf{p}} H_3^M(\mathbf{q}, \mathbf{p}, \mathbf{y}_q) = \mathbf{M}^{-1}\mathbf{p} \tag{7a}$$

$$\dot{\mathbf{p}} = -\nabla_{\mathbf{q}} H_3^M(\mathbf{q}, \mathbf{p}, \mathbf{y}_q) = -\nabla V(\mathbf{q}) - D\mathbf{g}^q(\mathbf{q})^T\mathbf{y}_q \tag{7b}$$

$$\mathbf{0} = \quad \nabla_{\mathbf{y}_q} H_3^M(\mathbf{q}, \mathbf{p}, \mathbf{y}_q) = \mathbf{g}^q(\mathbf{q}) \tag{7c}$$

It is well-known that the DAEs (7) have differentiation index three [2]. This can be easily seen by differentiating the configuration constraints a second time with respect to time, leading to

$$\frac{d}{dt}\mathbf{g}^v(\mathbf{q}, \mathbf{p}) = \partial_{\mathbf{q}}\mathbf{g}^v(\mathbf{q}, \mathbf{p})\dot{\mathbf{q}} + \partial_{\mathbf{p}}\mathbf{g}^v(\mathbf{q}, \mathbf{p})\dot{\mathbf{p}} = \mathbf{0}$$

Substituting (7a) and (7b) into the last equation yields

$$\mathbf{A}(\mathbf{q})\mathbf{y}_q = \mathbf{b}(\mathbf{q}, \mathbf{p}) \tag{8}$$

where

$$\mathbf{b}(\mathbf{q}, \mathbf{p}) = \partial_{\mathbf{q}}\mathbf{g}^v(\mathbf{q}, \mathbf{p})\mathbf{M}^{-1}\mathbf{p} - \partial_{\mathbf{p}}\mathbf{g}^v(\mathbf{q}, \mathbf{p})\nabla V(\mathbf{q}) \tag{9}$$

and matrix $\mathbf{A}(\mathbf{q})$ has been introduced in (3). Since matrix $\mathbf{A}(\mathbf{q})$ is non-singular, multiplier $\mathbf{y}_q$ can be expressed as

$$\mathbf{y}_q(\mathbf{q}, \mathbf{p}) = \mathbf{A}^{-1}(\mathbf{q})\mathbf{b}(\mathbf{q}, \mathbf{p}) \tag{10}$$

A third time differentiation yields a differential equation for $\mathbf{y}_q$. This confirms that the DAEs (7) have index three.

### 2.2. The state equations as stabilized index-2 DAEs

Alternatively to the index-3 DAEs (7) the equations of motion can be written as stabilized index-2 DAEs relying on the augmented mechanical Hamiltonian

$$H_2^M(\mathbf{q}, \mathbf{p}, \mathbf{y}_q, \mathbf{y}_v) = T(\mathbf{p}) + V(\mathbf{q}) + \mathbf{y}_q^T\mathbf{g}^q(\mathbf{q}) + \mathbf{y}_v^T\mathbf{g}^v(\mathbf{q}, \mathbf{p}) \tag{11}$$

where $\mathbf{y}_v \in \mathbb{R}^m$ are additional Lagrangian multipliers associated with the constraints (2) on velocity level. Now, instead of (7), we get

$$\dot{\mathbf{q}} = \quad \nabla_{\mathbf{p}} H_2^M(\mathbf{q}, \mathbf{p}, \mathbf{y}_q, \mathbf{y}_v) = \mathbf{M}^{-1}\mathbf{p} + \partial_{\mathbf{p}}\mathbf{g}^v(\mathbf{q}, \mathbf{p})^T\mathbf{y}_v \tag{12a}$$

$$\dot{\mathbf{p}} = -\nabla_{\mathbf{q}} H_2^M(\mathbf{q}, \mathbf{p}, \mathbf{y}_q, \mathbf{y}_v) = -\nabla V(\mathbf{q}) - D\mathbf{g}^q(\mathbf{q})^T\mathbf{y}_q - \partial_{\mathbf{q}}\mathbf{g}^v(\mathbf{q}, \mathbf{p})^T\mathbf{y}_v \tag{12b}$$

$$\mathbf{0} = \quad \nabla_{\mathbf{y}_q} H_2^M(\mathbf{q}, \mathbf{p}, \mathbf{y}_q, \mathbf{y}_v) = \mathbf{g}^q(\mathbf{q}) \tag{12c}$$

$$\mathbf{0} = \quad \nabla_{\mathbf{y}_v} H_2^M(\mathbf{q}, \mathbf{p}, \mathbf{y}_q, \mathbf{y}_v) = \mathbf{g}^v(\mathbf{q}, \mathbf{p}) \tag{12d}$$

The above DAEs yield an index reduction in the spirit of the often used GGL stabilization [5]. In particular, the DAEs (12) have differentiation index two [29,30]. This can be easily seen by differentiating the algebraic constraints in (12) with respect to time. This yields the consistency condition

$$\frac{d}{dt}\begin{bmatrix}\mathbf{g}^q(\mathbf{q}) \\ \mathbf{g}^v(\mathbf{q}, \mathbf{p})\end{bmatrix} = \begin{bmatrix}D\mathbf{g}^q(\mathbf{q}) & \mathbf{0} \\ \partial_{\mathbf{q}}\mathbf{g}^v(\mathbf{q}, \mathbf{p}) & \partial_{\mathbf{p}}\mathbf{g}^v(\mathbf{q}, \mathbf{p})\end{bmatrix}\begin{bmatrix}\dot{\mathbf{q}} \\ \dot{\mathbf{p}}\end{bmatrix} = \mathbf{0} \tag{13}$$

Now, the differential part of the DAEs (12) can be substituted into the last equation. To this end, we write (12a) and (12b) in the form

$$\begin{bmatrix}\dot{\mathbf{q}} \\ \dot{\mathbf{p}}\end{bmatrix} = \begin{bmatrix}\mathbf{M}^{-1}\mathbf{p} \\ -\nabla V(\mathbf{q})\end{bmatrix} - \begin{bmatrix}\mathbf{0} & -\partial_{\mathbf{p}}\mathbf{g}^v(\mathbf{q}, \mathbf{p})^T \\ D\mathbf{g}^q(\mathbf{q})^T & \partial_{\mathbf{q}}\mathbf{g}^v(\mathbf{q}, \mathbf{p})^T\end{bmatrix}\begin{bmatrix}\mathbf{y}_q \\ \mathbf{y}_v\end{bmatrix} \tag{14}$$

Inserting the last equation into (13), a straightforward calculation yields

$$\begin{bmatrix}\mathbf{0} & -\mathbf{A}(\mathbf{q}) \\ \mathbf{A}(\mathbf{q}) & \mathbf{C}(\mathbf{q}, \mathbf{p})\end{bmatrix}\begin{bmatrix}\mathbf{y}_q \\ \mathbf{y}_v\end{bmatrix} = \begin{bmatrix}\mathbf{g}^v(\mathbf{q}, \mathbf{p}) \\ \mathbf{b}(\mathbf{q}, \mathbf{p})\end{bmatrix} \tag{15}$$

where the skew-symmetric matrix $\mathbf{C}$ is given by

$$\mathbf{C}(\mathbf{q}, \mathbf{p}) = \partial_{\mathbf{p}}\mathbf{g}^v\partial_{\mathbf{q}}\mathbf{g}^{v^T} - \partial_{\mathbf{q}}\mathbf{g}^v\partial_{\mathbf{p}}\mathbf{g}^{v^T} \tag{16}$$

To obtain (15), $\partial_{\mathbf{p}}\mathbf{g}^v = D\mathbf{g}^q\mathbf{M}^{-1}$ has been used together with matrix $\mathbf{A}$ and vector $\mathbf{b}$, which have been introduced in (3) and (9), respectively. Now, the first line of (15) yields $\mathbf{y}_v = \mathbf{0}$, due to (12d) and the non-singularity of matrix $\mathbf{A}$. Moreover, the second line of (15) yields result (8). To summarize, in the continuous setting the DAEs (12) imply that $\mathbf{y}_v = \mathbf{0}$, and the DAEs (12) reduce to those in (7). However, in the discrete setting, the additional multipliers $\mathbf{y}_v$ serve the purpose to enforce the constraints (12d) on velocity level.

**Table 1**
Index-3 state DAEs.

Compact form

$$\dot{\mathbf{x}} = \mathbf{f}_3(\mathbf{x}, \mathbf{y}_3, \mathbf{u})$$
$$\mathbf{0} = \mathbf{g}_3(\mathbf{x})$$

Present quantities

$$\mathbf{x} = \begin{bmatrix} \mathbf{q} \\ \mathbf{p} \end{bmatrix} \qquad \mathbf{y}_3 = \mathbf{y}_q \qquad \mathbf{g}_3 = \mathbf{g}^q(\mathbf{q})$$

Compact r.h.s of the ODE

$$\mathbf{f}_3 = \begin{bmatrix} \mathbf{f}_3^{\mathbf{q}} \\ \mathbf{f}_3^{\mathbf{p}} \end{bmatrix} = \begin{bmatrix} \mathbf{M}^{-1}\mathbf{p} \\ -\nabla V(\mathbf{q}) - D\mathbf{g}^q(\mathbf{q})^T \mathbf{y}_q + \mathbf{B}(\mathbf{q})\mathbf{u} \end{bmatrix}$$

### 2.3. The controlled hamiltonian state equations

The two alternative versions of the state equations outlined above can be written in a unified way by introducing the augmented mechanical Hamiltonian

$$H_i^M(\mathbf{q}, \mathbf{p}, \mathbf{y}_i) = T(\mathbf{p}) + V(\mathbf{q}) + \mathbf{y}_i^T \mathbf{g}_i(\mathbf{q}, \mathbf{p}) \tag{17}$$

Here, index $i$ labels the respective Hamiltonians (5) and (11) and consequently hints at the index of the resulting DAEs. Accordingly, one may choose either $i = 3$ or $i = 2$. For the case $i = 3$ the Lagrange multipliers and constraint functions are

$$\mathbf{y}_3 = \mathbf{y}_q \qquad \mathbf{g}_3(\mathbf{q}, \mathbf{p}) = \mathbf{g}^q(\mathbf{q}) \tag{18}$$

whereas for the case $i = 2$,

$$\mathbf{y}_2 = \begin{bmatrix} \mathbf{y}_q \\ \mathbf{y}_v \end{bmatrix} \qquad \mathbf{g}_2(\mathbf{q}, \mathbf{p}) = \begin{bmatrix} \mathbf{g}^q(\mathbf{q}) \\ \mathbf{g}^v(\mathbf{q}, \mathbf{p}) \end{bmatrix} \tag{19}$$

As outlined above, the corresponding DAEs have either index $i = 3$ or $i = 2$. Taking into account the additional influence of actuating forces on the system, the controlled Hamiltonian state equations are given by

$$\dot{\mathbf{q}} = \nabla_{\mathbf{p}} H_i^M(\mathbf{q}, \mathbf{p}, \mathbf{y}_i) \tag{20a}$$
$$\dot{\mathbf{p}} = -\nabla_{\mathbf{q}} H_i^M(\mathbf{q}, \mathbf{p}, \mathbf{y}_i) + \mathbf{B}(\mathbf{q})\mathbf{u} \tag{20b}$$
$$\mathbf{0} = \nabla_{\mathbf{y}_i} H_i^M(\mathbf{q}, \mathbf{p}, \mathbf{y}_i) \tag{20c}$$

where $\mathbf{u} \in \mathcal{U} \subseteq \mathbb{R}^n$ are the control inputs and $\mathbf{B}$ is the control distribution matrix. The controlled state Eqs. (20) can be written in the more compact from

$$\dot{\mathbf{q}} = \mathbf{f}_i^{\mathbf{q}}(\mathbf{q}, \mathbf{p}, \mathbf{y}_i) \tag{21a}$$
$$\dot{\mathbf{p}} = \mathbf{f}_i^{\mathbf{p}}(\mathbf{q}, \mathbf{p}, \mathbf{y}_i, \mathbf{u}) \tag{21b}$$
$$\mathbf{0} = \mathbf{g}_i(\mathbf{q}, \mathbf{p}) \tag{21c}$$

for $i \in \{2, 3\}$. Eventually, introducing the phase space vector $\mathbf{x} = (\mathbf{q}, \mathbf{p})$, the state Eqs. (21) can be rewritten as

$$\dot{\mathbf{x}} = \mathbf{f}_i(\mathbf{x}, \mathbf{y}_i, \mathbf{u}) \tag{22a}$$
$$\mathbf{0} = \mathbf{g}_i(\mathbf{x}) \tag{22b}$$

for $i \in \{2, 3\}$. Since $\mathbf{x} \in \mathcal{T}^*\mathcal{M} \equiv \mathcal{P}$ represents the state of the mechanical system in phase space $\mathcal{P}$, $\mathbf{x} \in \mathcal{P}$ is also called state vector in the sequel. For later reference, Tables 1 and 2 provide a summary of the present DAEs governing the motion of controlled mechanical systems subject to holonomic constraints. These DAEs play the role of state equations in the optimal control problem dealt with in the sequel.

For later use, we eventually provide the formulas for the Lagrange multipliers in terms of the states and the controls, i.e. $\mathbf{y}_i = \mathbf{y}_i(\mathbf{x}, \mathbf{u})$ ($i \in \{2, 3\}$). In particular, for $i = 3$, repeating the calculation that led to (8), we obtain

$$\mathbf{A}(\mathbf{q})\mathbf{y}_3 = \mathbf{b}(\mathbf{q}, \mathbf{p}) + D\mathbf{g}^q(\mathbf{q})\mathbf{M}^{-1}\mathbf{B}(\mathbf{q})\mathbf{u} \tag{23}$$

**Table 2**
Stabilized index-2 state DAEs.

Compact form

$$\dot{\mathbf{x}} = \mathbf{f}_2(\mathbf{x}, \mathbf{y}_2, \mathbf{u})$$
$$\mathbf{0} = \mathbf{g}_2(\mathbf{x})$$

Present quantities

$$\mathbf{x} = \begin{bmatrix} \mathbf{q} \\ \mathbf{p} \end{bmatrix} \qquad \mathbf{y}_2 = \begin{bmatrix} \mathbf{y}_q \\ \mathbf{y}_v \end{bmatrix} \qquad \mathbf{g}_2 = \begin{bmatrix} \mathbf{g}^q(\mathbf{q}) \\ \mathbf{g}^v(\mathbf{q}, \mathbf{p}) \end{bmatrix}$$

Compact r.h.s of the ODE

$$\mathbf{f}_2 = \begin{bmatrix} \mathbf{f}_2^{\mathbf{q}} \\ \mathbf{f}_2^{\mathbf{p}} \end{bmatrix} = \begin{bmatrix} \mathbf{M}^{-1}\mathbf{p} + \partial_{\mathbf{p}}\mathbf{g}^v(\mathbf{q}, \mathbf{p})^T \mathbf{y}_v \\ -\nabla V(\mathbf{q}) - D\mathbf{g}^q(\mathbf{q})^T \mathbf{y}_q - \partial_{\mathbf{q}}\mathbf{g}^v(\mathbf{q}, \mathbf{p})^T \mathbf{y}_v + \mathbf{B}(\mathbf{q})\mathbf{u} \end{bmatrix}$$

Consequently, multiplier $\mathbf{y}_3$ can be expressed as $\mathbf{y}_3 = \mathbf{y}_3(\mathbf{x}, \mathbf{u})$. Similarly, including the presence of controls in (15) yields

$$\begin{bmatrix} \mathbf{0} & -\mathbf{A}(\mathbf{q}) \\ \mathbf{A}(\mathbf{q}) & \mathbf{C}(\mathbf{q}, \mathbf{p}) \end{bmatrix} \mathbf{y}_2 = \begin{bmatrix} \mathbf{g}^v(\mathbf{q}, \mathbf{p}) \\ \mathbf{b}(\mathbf{q}, \mathbf{p}) \end{bmatrix} + \begin{bmatrix} \mathbf{0} \\ D\mathbf{g}^q(\mathbf{q})\mathbf{M}^{-1}\mathbf{B}(\mathbf{q})\mathbf{u} \end{bmatrix} \tag{24}$$

Thus, multiplier $\mathbf{y}_2$ can be expressed as $\mathbf{y}_2 = \mathbf{y}_2(\mathbf{x}, \mathbf{u})$.

## 3. The optimal control problem

Next we address the optimal control problem for constrained mechanical systems. In particular, we seek to minimize the cost functional $S[\mathbf{x}, \mathbf{y}_i, \mathbf{u}]$ subject to the state DAEs (22) during the fixed time interval $[t_0, t_f]$. We assume that the states at the boundaries are prescribed. That is, $\mathbf{x}(t_0) = \bar{\mathbf{x}}_0$ and $\mathbf{x}(t_f) = \bar{\mathbf{x}}_f$, where $\bar{\mathbf{x}}_0, \bar{\mathbf{x}}_f \in \mathcal{T}^*\mathcal{Q}$ are given. The optimal control problem can be stated as follows.

Minimize

$$S[\mathbf{x}, \mathbf{y}_i, \mathbf{u}] = \int_{t_0}^{t_f} C(\mathbf{x}, \mathbf{y}_i, \mathbf{u})\, \mathrm{d}t \tag{25a}$$

subject to

$$\dot{\mathbf{x}} = \mathbf{f}_i(\mathbf{x}, \mathbf{y}_i, \mathbf{u}) \tag{25b}$$
$$\mathbf{0} = \mathbf{g}_i(\mathbf{x}) \tag{25c}$$
$$\mathbf{x}(t_0) = \bar{\mathbf{x}}_0 \tag{25d}$$
$$\mathbf{x}(t_f) = \bar{\mathbf{x}}_f \tag{25e}$$

In (25a), $C$ is the prescribed cost density function. In the present work we put the focus on unbounded controls $\mathbf{u} \in \mathcal{U} \subseteq \mathbb{R}^n$. As before, index $i \in \{2, 3\}$ serves the purpose to distinguish the two alternative state equations introduced in the last section.

### 3.1. Optimality conditions according to the maximum principle

A maximum principle for optimal control problems, in which the state equations are given by nonlinear index-3 and index-2 DAEs has been devised in [12], see also [4]. Accordingly, the necessary optimality conditions can be formulated in terms of an optimal control Hamiltonian given by

$$\mathcal{H}_i(\mathbf{x}, \mathbf{y}_i, \mathbf{u}, \lambda, \boldsymbol{\eta}_i) = \lambda^T \mathbf{f}_i(\mathbf{x}, \mathbf{y}_i, \mathbf{u}) + \boldsymbol{\eta}_i^T \widetilde{\mathbf{g}}_i(\mathbf{x}, \mathbf{y}_i, \mathbf{u}) - C(\mathbf{x}, \mathbf{y}_i, \mathbf{u}) \tag{26}$$

Here, $\lambda$ and $\boldsymbol{\eta}_i$ ($i \in \{2, 3\}$) are adjoint variables of appropriate dimensions. If the underlying state DAEs have index $i = 3$, function $\widetilde{\mathbf{g}}_3$ in Hamiltonian (26) is given by

$$\widetilde{\mathbf{g}}_3(\mathbf{x}, \mathbf{y}_3, \mathbf{u}) = D\mathbf{g}^v(\mathbf{x})\mathbf{f}_3(\mathbf{x}, \mathbf{y}_3, \mathbf{u}) \tag{27a}$$
$$= \partial_{\mathbf{q}}\mathbf{g}^v(\mathbf{q}, \mathbf{p})\mathbf{f}_3^{\mathbf{q}}(\mathbf{q}, \mathbf{p}) + \partial_{\mathbf{p}}\mathbf{g}^v(\mathbf{q}, \mathbf{p})\mathbf{f}_3^{\mathbf{p}}(\mathbf{q}, \mathbf{p}, \mathbf{y}_3, \mathbf{u}) \tag{27b}$$

Correspondingly, in Hamiltonian (26), the algebraic adjoint variables $\boldsymbol{\eta}_3 \in \mathbb{R}^m$.

If the underlying state DAEs have index $i = 2$, function $\widetilde{\mathbf{g}}_2$ in Hamiltonian (26) is given by

$$\widetilde{\mathbf{g}}_2(\mathbf{x}, \mathbf{y}_2, \mathbf{u}) = D\mathbf{g}_2(\mathbf{x})\mathbf{f}_2(\mathbf{x}, \mathbf{y}_2, \mathbf{u}) \tag{28a}$$

$$= \begin{bmatrix} D\mathbf{g}^q(\mathbf{q}) & \mathbf{0} \\ \partial_{\mathbf{q}}\mathbf{g}^v(\mathbf{q},\mathbf{p}) & \partial_{\mathbf{p}}\mathbf{g}^v(\mathbf{q},\mathbf{p}) \end{bmatrix} \begin{bmatrix} \mathbf{f}_2^{\mathbf{q}}(\mathbf{q},\mathbf{p},\mathbf{y}_2) \\ \mathbf{f}_2^{\mathbf{p}}(\mathbf{q},\mathbf{p},\mathbf{y}_2,\mathbf{u}) \end{bmatrix} \tag{28b}$$

Correspondingly, in Hamiltonian (26), the algebraic adjoint variables $\boldsymbol{\eta}_2 \in \mathbb{R}^{2m}$. The necessary conditions of optimality consist of the state equations in (25), along with the optimality condition

$$\mathbf{0} = \nabla_{\mathbf{u}} \mathcal{H}_i(\mathbf{x},\mathbf{y}_i,\mathbf{u},\lambda,\boldsymbol{\eta}_i) \tag{29a}$$

and the adjoint DAEs

$$\dot{\lambda} = -\nabla_{\mathbf{x}} \mathcal{H}_i(\mathbf{x},\mathbf{y}_i,\mathbf{u},\lambda,\boldsymbol{\eta}_i) \tag{29b}$$

$$\mathbf{0} = \nabla_{\mathbf{y}_i} \mathcal{H}_i(\mathbf{x},\mathbf{y}_i,\mathbf{u},\lambda,\boldsymbol{\eta}_i) \tag{29c}$$

### 3.2. Optimality conditions according to the common approach

As observed in [12], it is common belief that the standard maximum principle for ODEs can be applied to optimal control problems subject to state DAEs. As outlined in Section 1, this observation still persists in the literature on computational mechanics. The common approach is based on the introduction of a Hamiltonian of the form

$$\overline{\mathcal{H}}_i(\mathbf{x},\mathbf{y}_i,\mathbf{u},\lambda,\boldsymbol{\eta}_i) = \lambda^T \mathbf{f}_i(\mathbf{x},\mathbf{y}_i,\mathbf{u}) + \boldsymbol{\eta}_i^T \mathbf{g}_i(\mathbf{x}) - C(\mathbf{x},\mathbf{y}_i,\mathbf{u}) \tag{30}$$

In contrast to Hamiltonian (26), the constraint functions $\mathbf{g}_i$ are directly used in (30) instead of $\widetilde{\mathbf{g}}_i$ in (26). Of course, this difference affects the form of the optimality conditions which still result from (29) by replacing $\mathcal{H}_i$ with $\overline{\mathcal{H}}_i$. Apart from that, there is another crucial difference: Similar to the standard maximum principle for ODEs, the state equations in (25) can be derived from the Hamiltonian (30) according to

$$\dot{\mathbf{x}} = \nabla_{\lambda} \overline{\mathcal{H}}_i(\mathbf{x},\mathbf{y}_i,\mathbf{u},\lambda,\boldsymbol{\eta}_i) \tag{31a}$$

$$\mathbf{0} = \nabla_{\boldsymbol{\eta}_i} \overline{\mathcal{H}}_i(\mathbf{x},\mathbf{y}_i,\mathbf{u},\lambda,\boldsymbol{\eta}_i) \tag{31b}$$

Correspondingly, the optimality conditions now have an underlying variational structure in the sense that they can be derived from an augmented cost functional given by

$$\overline{S}_i = \int_{t_0}^{t_f} C(\mathbf{x},\mathbf{y}_i,\mathbf{u}) + \lambda^T \left(\dot{\mathbf{x}} - \mathbf{f}_i(\mathbf{x},\mathbf{y}_i,\mathbf{u})\right) - \boldsymbol{\eta}_i^T \mathbf{g}_i(\mathbf{x}) \, \mathrm{d}t \tag{32}$$

Employing Hamiltonian (30), the augmented cost functional $\overline{S}_i$ can be recast in the form

$$\overline{S}_i = \int_{t_0}^{t_f} \lambda^T \dot{\mathbf{x}} - \overline{\mathcal{H}}_i(\mathbf{x},\mathbf{y}_i,\mathbf{u},\lambda,\boldsymbol{\eta}_i) \, \mathrm{d}t \tag{33}$$

It can be easily verified that imposing stationary of the augmented cost functional $\overline{S}_i$ yields as Euler–Lagrange equations the necessary conditions of optimality (29) along with the state DAEs (31).

**Remark 1.** While the optimal control formulation according to the common approach has an underlying variational structure that hinges on the existence of the augmented cost functional $\overline{S}_i$, this is not the case for the formulation based on the maximum principle dealt with in Section 3.1. In particular, employing Hamiltonian (26) instead of (30) yields the functional

$$S_i = \int_{t_0}^{t_f} \lambda^T \dot{\mathbf{x}} - \mathcal{H}_i(\mathbf{x},\mathbf{y}_i,\mathbf{u},\lambda,\boldsymbol{\eta}_i) \, \mathrm{d}t \tag{34}$$

whose Euler–Lagrange equation

$$\mathbf{0} = \nabla_{\boldsymbol{\eta}_i} \mathcal{H}_i(\mathbf{x},\mathbf{y}_i,\mathbf{u},\lambda,\boldsymbol{\eta}_i) \neq \mathbf{g}_i(\mathbf{x}) \tag{35}$$

does not yield the constraints (25c) of the underlying state DAEs. This structural discrepancy of the formulation based on the maximum principle impairs the design of numerical methods based on the direct approach [20]. In essence, the direct approach 'first discretize then optimize' relies on the discretization of variational functionals such as (33) and (34). We shall dwell further on this point in Section 5.

### 3.3. The adjoint DAEs and the index of the adjoint variables

In this section we focus on the adjoint DAEs and the index of the adjoint variables, depending on whether the adjoint DAEs emanate from the maximum principle or the common approach. For simplicity of exposition, we assume that the density cost function is given by $C = C(\mathbf{u}) = \frac{1}{2}\mathbf{u}^T\mathbf{E}\mathbf{u}$, where matrix $\mathbf{E}$ is assumed to be positive definite.

#### 3.3.1. Adjoint DAEs according to the maximum principle

As mentioned in Section 3.1, the entire system of DAEs to be considered is comprised of the state equations in (25), optimality condition (29a) and adjoint Eqs. (29b) and (29c).

We provide the adjoint DAEs emanating from (29b) and (29c) in more detail by employing Hamiltonian (26). Moreover, we show that the adjoint equations form DAEs of index 1 for the adjoint variables, independent from index $i \in \{2,3\}$ of the underlying state DAEs. If we partition the differential adjoint variables $\lambda = \left(\lambda_{\mathbf{q}}, \lambda_{\mathbf{p}}\right)$ in analogy to the state variables $\mathbf{x} = (\mathbf{q}, \mathbf{p})$, for $i = 3$, Hamiltonian (26) can be written as

$$\mathcal{H}_3 = \lambda_{\mathbf{q}}^T \mathbf{f}_3^{\mathbf{q}} + \lambda_{\mathbf{p}}^T \mathbf{f}_3^{\mathbf{p}} + \boldsymbol{\eta}_3^T \widetilde{\mathbf{g}}_3 - C \tag{36}$$

Now, the differential part (29b) of the adjoint DAEs yields

$$\dot{\lambda}_{\mathbf{q}} = -\partial_{\mathbf{q}} \mathbf{f}_3^{\mathbf{p}^T} \lambda_{\mathbf{p}} - \partial_{\mathbf{q}} \widetilde{\mathbf{g}}_3^T \boldsymbol{\eta}_3 \tag{37a}$$

$$\dot{\lambda}_{\mathbf{p}} = -\partial_{\mathbf{p}} \mathbf{f}_3^{\mathbf{q}^T} \lambda_{\mathbf{q}} - \partial_{\mathbf{p}} \widetilde{\mathbf{g}}_3^T \boldsymbol{\eta}_3 \tag{37b}$$

while the algebraic part (29c) leads to

$$\mathbf{0} = \partial_{\mathbf{y}_3} \mathbf{f}_3^{\mathbf{p}^T} \lambda_{\mathbf{p}} + \partial_{\mathbf{y}_3} \widetilde{\mathbf{g}}_3^T \boldsymbol{\eta}_3$$

or

$$\mathbf{0} = D\mathbf{g}^q(\mathbf{q}) \lambda_{\mathbf{p}} - \mathbf{A}(\mathbf{q}) \boldsymbol{\eta}_3$$

where matrix $\mathbf{A}(\mathbf{q})$ has been introduced in (3). Accordingly,

$$\boldsymbol{\eta}_3 = \mathbf{A}^{-1} D\mathbf{g}^q(\mathbf{q}) \lambda_{\mathbf{p}} \tag{38}$$

such that algebraic adjoint variable $\boldsymbol{\eta}_3$ can be expressed as $\boldsymbol{\eta}_3 = \boldsymbol{\eta}_3(\mathbf{q}, \lambda_{\mathbf{p}})$, which implies that the adjoint equations form DAEs of index 1 for the adjoint variables. For completeness, optimality condition (29a) gives rise to the relationship

$$\mathbf{0} = \partial_{\mathbf{u}} \mathcal{H}_3 = \lambda_{\mathbf{p}}^T \partial_{\mathbf{u}} \mathbf{f}_3^{\mathbf{p}} + \boldsymbol{\eta}_3^T \partial_{\mathbf{u}} \widetilde{\mathbf{g}}_3 - \partial_{\mathbf{u}} C$$

leading to

$$\mathbf{E}\mathbf{u} = \mathbf{B}^T \left( \lambda_{\mathbf{p}} + \mathbf{M}^{-1} D\mathbf{g}^{q^T} \boldsymbol{\eta}_3 \right) \tag{39}$$

Similarly, for $i = 2$, adjoint Eq. (29c) gives rise to

$$\mathbf{0} = \partial_{\mathbf{y}_2} \mathcal{H}_2 = \lambda^T \partial_{\mathbf{y}_2} \mathbf{f}_2 + \boldsymbol{\eta}_2^T \partial_{\mathbf{y}_2} \widetilde{\mathbf{g}}_2$$

Now, a straightforward calculation yields

$$\begin{bmatrix} \mathbf{0} & \mathbf{A} \\ -\mathbf{A} & \mathbf{C}^T \end{bmatrix} \boldsymbol{\eta}_2 = - \begin{bmatrix} \mathbf{0} & D\mathbf{g}^q \\ -\partial_{\mathbf{p}} \mathbf{g}^v & \partial_{\mathbf{q}} \mathbf{g}^v \end{bmatrix} \lambda \tag{40}$$

where matrices $\mathbf{A}$ and $\mathbf{C}$ have been introduced in (3) and (16), respectively. Accordingly, since matrix $\mathbf{A}$ is non-singular, algebraic adjoint variable $\boldsymbol{\eta}_2$ can be expressed as $\boldsymbol{\eta}_2 = \boldsymbol{\eta}_2(\mathbf{x}, \lambda)$, which implies that the adjoint equations form DAEs of index 1 for the adjoint variables. For completeness, optimality condition (29a) gives rise to the relationship

$$\mathbf{0} = \partial_{\mathbf{u}} \mathcal{H}_2 = \lambda^T \partial_{\mathbf{u}} \mathbf{f}_2 + \boldsymbol{\eta}_2^T \partial_{\mathbf{u}} \widetilde{\mathbf{g}}_2 - \partial_{\mathbf{u}} C$$

leading to

$$\mathbf{E}\mathbf{u} = \mathbf{B}^T \left( \lambda_{\mathbf{p}} + \mathbf{M}^{-1} D\mathbf{g}^{q^T} \boldsymbol{\eta}_2^{\mathbf{a}} \right) \tag{41}$$

where the algebraic adjoint variables have been partitioned according to $\boldsymbol{\eta}_2 = \left(\boldsymbol{\eta}_2^{\mathbf{v}}, \boldsymbol{\eta}_2^{\mathbf{a}}\right)$.

### 3.3.2. Adjoint DAEs according to the common approach

According to Section 3.2, the entire system of DAEs to be considered is comprised of the state equations in (25), optimality condition (29a) and adjoint Eqs. (29b) and (29c), where now Hamiltonian (30) has to be applied.

We consider the adjoint DAEs emanating from (29b) and (29c) by using Hamiltonian $\overline{\mathcal{H}}_i$ defined in (30). In particular, we show that the adjoint equations form DAEs of index $i \in \{2,3\}$ for the adjoint variables.

Starting with $i = 3$, Hamiltonian (30) reads

$$\overline{\mathcal{H}}_3 = \lambda_{\mathbf{q}}^T \mathbf{f}_3^{\mathbf{q}} + \lambda_{\mathbf{p}}^T \mathbf{f}_3^{\mathbf{p}} + \boldsymbol{\eta}_3^T \mathbf{g}_3 - C \tag{42}$$

Now, the differential part (29b) of the adjoint DAEs yields

$$\dot{\lambda}_{\mathbf{q}} = -\partial_{\mathbf{q}} \mathbf{f}_3^{\mathbf{p}^T} \lambda_{\mathbf{p}} - D\mathbf{g}^{q^T} \boldsymbol{\eta}_3 \tag{43a}$$

$$\dot{\lambda}_{\mathbf{p}} = -\partial_{\mathbf{p}} \mathbf{f}_3^{\mathbf{q}^T} \lambda_{\mathbf{q}} \tag{43b}$$

Optimality condition (29a) gives rise to the relationship

$$\mathbf{0} = \partial_{\mathbf{u}} \overline{\mathcal{H}}_3 = \lambda_{\mathbf{p}}^T \partial_{\mathbf{u}} \mathbf{f}_3^{\mathbf{p}} - \partial_{\mathbf{u}} C$$

leading to

$$\mathbf{E}\mathbf{u} = \mathbf{B}^T \lambda_{\mathbf{p}} \tag{44}$$

Accordingly, since $\mathbf{E}$ is invertible, the control vector $\mathbf{u}$ can be expressed in terms of the adjoint variables $\lambda_{\mathbf{p}}$. Algebraic part (29c) of the adjoint DAEs leads to

$$\mathbf{0} = \partial_{\mathbf{y}_3} \mathbf{f}_3^{\mathbf{p}^T} \lambda_{\mathbf{p}} = -D\mathbf{g}^q \lambda_{\mathbf{p}}$$

Differentiating the last equation with respect to time yields

$$\mathbf{0} = \frac{d}{dt} (D\mathbf{g}^q) \lambda_{\mathbf{p}} + D\mathbf{g}^q \dot{\lambda}_{\mathbf{p}}$$

Inserting (43b) into the last equation gives

$$\mathbf{0} = \frac{d}{dt} (D\mathbf{g}^q) \lambda_{\mathbf{p}} - D\mathbf{g}^q \mathbf{M}^{-1} \lambda_{\mathbf{q}}$$

A second time differentiation of the last equation yields, after a straightforward calculation which takes into account (43),

$$\mathbf{A}\boldsymbol{\eta}_3 = \mathbf{h}(\mathbf{x}, \mathbf{y}_3, \mathbf{u}, \lambda) \tag{45}$$

where matrix $\mathbf{A}$ has been introduced in (3) and function $\mathbf{h}$ collects the remaining terms. Taking into account (23) and (44), the last equation implies that algebraic adjoint variables $\boldsymbol{\eta}_3$ can be expressed as $\boldsymbol{\eta}_3 = \boldsymbol{\eta}_3(\mathbf{x}, \lambda)$. Accordingly, the adjoint equations form DAEs of index 3 for the adjoint variables, which equals the index of the underlying state DAEs.

For $i = 2$, the differential part (29b) of the adjoint DAEs yields

$$\dot{\lambda} = -\partial_{\mathbf{x}} \mathbf{f}_2^T \lambda - \partial_{\mathbf{x}} \mathbf{g}_2^T \boldsymbol{\eta}_2 \tag{46}$$

while the optimality condition (29a) gives rise to the relationship

$$\mathbf{0} = \partial_{\mathbf{u}} \overline{H}_2 = \lambda_{\mathbf{p}}^T \partial_{\mathbf{u}} \mathbf{f}_2^{\mathbf{p}} - \partial_{\mathbf{u}} C$$

which again yields

$$\mathbf{E}\mathbf{u} = \mathbf{B}^T \lambda_{\mathbf{p}} \tag{47}$$

Algebraic part (29c) of the adjoint DAEs gives rise to

$$\mathbf{0} = \partial_{\mathbf{y}_2} \overline{H}_2 = \lambda^T \partial_{\mathbf{y}_2} \mathbf{f}_2 = \lambda^T \begin{bmatrix} \mathbf{0} & -\partial_{\mathbf{p}} \mathbf{g}^{v^T} \\ D\mathbf{g}^{q^T} & \partial_{\mathbf{q}} \mathbf{g}^{v^T} \end{bmatrix}$$

Differentiating the last equation with respect to time, and inserting (46), a straightforward calculation yields

$$\begin{bmatrix} \mathbf{0} & \mathbf{A} \\ -\mathbf{A} & \mathbf{C}^T \end{bmatrix} \boldsymbol{\eta}_2 = \hat{\mathbf{h}}(\mathbf{x}, \mathbf{y}_2, \mathbf{u}, \lambda) \tag{48}$$

where remaining terms have been collected in function $\hat{\mathbf{h}}$. Moreover, matrices $\mathbf{A}$ and $\mathbf{C}$ have been introduced in (3) and (16), respectively. The last equation together with (24) and (47) imply that the algebraic adjoint variables $\boldsymbol{\eta}_2$ can be expressed as $\boldsymbol{\eta}_2 = \boldsymbol{\eta}_2(\mathbf{x}, \lambda)$. Thus one may conclude that the adjoint equations form DAEs of index 2 for the adjoint variables, which equals the index of the underlying state DAEs.

## 4. Conservation properties of the optimal control problem

### 4.1. Conservation of generalized momentum maps

If the state equations of an optimal control problem assume the form of ODEs, it has been shown in [27] that symmetries of the underlying *uncontrolled* mechanical system are inherited by the optimal control problem, provided that the cost function also respects the symmetries. Symmetries of the optimal control problem give rise to the conservation of generalized momentum maps, which is in line with Noether's theorem [25,26]. Analogous observations hold for the optimal control of constrained mechanical systems whose motion is governed by DAEs. This will be shown in the sequel. Our presentation covers the two alternative optimal control formulations dealt with in the last section comprised of state DAEs with index $i \in \{2, 3\}$, and thus generalizes our previous work [28] that has been confined to the maximum principle and $i = 2$.

Consider the action of a Lie group $G$ on phase space $\mathcal{P}$ given by the smooth mapping $\Phi : G \times \mathcal{P} \to \mathcal{P}$ such that $\Phi_g(\mathbf{x}) = \Phi(g, \mathbf{x})$, for $g \in G$. Accordingly, $\Phi_g : \mathcal{P} \to \mathcal{P}$ for every $g \in G$. In particular, we consider the one-parameter subgroup $\{g^s = \exp(s\boldsymbol{\xi}) : s \in \mathbb{R}\} \subseteq G$, where $\boldsymbol{\xi}$ is a vector in the Lie algebra $\mathfrak{g}$ of $G$. Note that $\Phi(g^0, \mathbf{x}) = \mathbf{x}$. We further define the infinitesimal generator associated to $\boldsymbol{\xi} \in \mathfrak{g}$ at $\mathbf{x} \in \mathcal{P}$ by

$$\boldsymbol{\xi}_{\mathcal{P}}(\mathbf{x}) = \left. \frac{\mathrm{d}}{\mathrm{d}s} \right|_{s=0} \Phi_{g^s}(\mathbf{x}) \tag{49}$$

**Proposition 1.** *Provided that the following symmetry conditions*

$$\mathbf{f}_i(\Phi_{g^s}(\mathbf{x}), \mathbf{y}_i^s, \mathbf{u}^s) = D\Phi_{g^s}(\mathbf{x}) \mathbf{f}_i(\mathbf{x}, \mathbf{y}_i, \mathbf{u}) \tag{50a}$$

$$\mathbf{g}_i(\Phi_{g^s}(\mathbf{x})) = \mathbf{g}_i(\mathbf{x}) \tag{50b}$$

$$C(\boldsymbol{\Phi}_{g^s}(\mathbf{x}), \mathbf{y}_i^s, \mathbf{u}^s) = C(\mathbf{x}, \mathbf{y}_i, \mathbf{u}) \tag{50c}$$

*are satisfied for some* $\mathbf{u}^s$ *and* $\mathbf{y}_i^s$ *satisfying* $\mathbf{u}^0 = \mathbf{u}$ *and* $\mathbf{y}_i^0 = \mathbf{y}_i$*, generalized momentum maps of the form*

$$J_\xi(\mathbf{x}, \boldsymbol{\lambda}) = \boldsymbol{\lambda}^T \boldsymbol{\xi}_{\mathcal{P}}(\mathbf{x}) \tag{51}$$

*are conserved along solutions of the optimal control problem. This holds for* $i \in \{2, 3\}$ *and the two alternative optimal control formulations treated above.*

The proof of Proposition 1 is contained in the next two sections.

#### 4.1.1. Optimal control formulation based on the maximum principle

We start with the formulation of the optimal control problem according to the maximum principle dealt with in Section 3.1. We first show that symmetry conditions (50a) and (50b) imply that

$$\widetilde{\mathbf{g}}_i(\boldsymbol{\Phi}_{g^s}(\mathbf{x}), \mathbf{y}_i^s, \mathbf{u}^s) = \widetilde{\mathbf{g}}_i(\mathbf{x}, \mathbf{y}_i, \mathbf{u}) \tag{52}$$

for $i \in \{2, 3\}$. To see this, consider the derivative of (50b) with respect to time leading to

$$\frac{d}{dt}\mathbf{g}_i(\boldsymbol{\Phi}_{g^s}(\mathbf{x})) = D\mathbf{g}_i(\boldsymbol{\Phi}_{g^s}(\mathbf{x}))\frac{d}{dt}\boldsymbol{\Phi}_{g^s}(\mathbf{x}) = D\mathbf{g}_i(\boldsymbol{\Phi}_{g^s}(\mathbf{x}))D\boldsymbol{\Phi}_{g^s}(\mathbf{x})\dot{\mathbf{x}} = D\mathbf{g}_i(\mathbf{x})\dot{\mathbf{x}}$$

Note that the right-hand side of the last equation corresponds to the time derivative of the right-hand side of (50b). Inserting the state Eq. (22a) in the above equation yields

$$D\mathbf{g}_i(\boldsymbol{\Phi}_{g^s}(\mathbf{x}))D\boldsymbol{\Phi}_{g^s}(\mathbf{x})\mathbf{f}_i(\mathbf{x}, \mathbf{y}_i, \mathbf{u}) = D\mathbf{g}_i(\mathbf{x})\mathbf{f}_i(\mathbf{x}, \mathbf{y}_i, \mathbf{u})$$

Making use of symmetry condition (50a) on the left-hand side of the last equation gives

$$D\mathbf{g}_i(\boldsymbol{\Phi}_{g^s}(\mathbf{x}))\mathbf{f}_i(\boldsymbol{\Phi}_{g^s}(\mathbf{x}), \mathbf{y}_i^s, \mathbf{u}^s) = D\mathbf{g}_i(\mathbf{x})\mathbf{f}_i(\mathbf{x}, \mathbf{y}_i, \mathbf{u})$$

For $i = 2$, the last equation directly proofs (52), since $\widetilde{\mathbf{g}}_2$ is defined by $\widetilde{\mathbf{g}}_2(\mathbf{x}, \mathbf{y}_2, \mathbf{u}) = D\mathbf{g}_2(\mathbf{x})\mathbf{f}_2(\mathbf{x}, \mathbf{y}_2, \mathbf{u})$, see (28). For $i = 3$, the last equation implies $\mathbf{g}^v(\boldsymbol{\Phi}_{g^s}(\mathbf{x})) = \mathbf{g}^v(\mathbf{x})$, since the velocity-level constraint function introduced in (2) can be written as $\mathbf{g}^v(\mathbf{x}) = D\mathbf{g}_3(\mathbf{x})\mathbf{f}_3(\mathbf{x}, \mathbf{y}_3, \mathbf{u})$. Now, since $\widetilde{\mathbf{g}}_3(\mathbf{x}, \mathbf{y}_3, \mathbf{u}) = D\mathbf{g}^v(\mathbf{x})\mathbf{f}_3(\mathbf{x}, \mathbf{y}_3, \mathbf{u})$, c.f. (27), the above procedure can be repeated by replacing $\widetilde{\mathbf{g}}_i$ with $\mathbf{g}^v$, which proofs (52) for $i = 3$.

Strictly speaking, the proof of Proposition 1 only requires the infinitesimal versions of the symmetry conditions (50a), (52) and (50c). Starting with (50a), we get

$$\frac{\mathrm{d}}{\mathrm{d}s}\bigg|_{s=0} \mathbf{f}_i(\boldsymbol{\Phi}_{g^s}(\mathbf{x}), \mathbf{y}_i^s, \mathbf{u}^s) = \frac{\mathrm{d}}{\mathrm{d}s}\bigg|_{s=0} D\boldsymbol{\Phi}_{g^s}(\mathbf{x})\mathbf{f}_i(\mathbf{x}, \mathbf{y}_i, \mathbf{u})$$

Now, a straightforward calculation based on the last equation yields

$$\begin{aligned} \partial_{\mathbf{x}}\mathbf{f}_i(\mathbf{x}, \mathbf{y}_i, \mathbf{u})\boldsymbol{\xi}_{\mathcal{P}}(\mathbf{x}) \quad &+ \quad \partial_{\mathbf{y}_i}\mathbf{f}_i(\mathbf{x}, \mathbf{y}_i, \mathbf{u}) \left.\frac{\mathrm{d}}{\mathrm{d}s}\right|_{s=0} \mathbf{y}_i^s \\ &+ \quad \partial_{\mathbf{u}}\mathbf{f}_i(\mathbf{x}, \mathbf{y}_i, \mathbf{u}) \left.\frac{\mathrm{d}}{\mathrm{d}s}\right|_{s=0} \mathbf{u}^s = D\boldsymbol{\xi}_{\mathcal{P}}(\mathbf{x})\mathbf{f}_i(\mathbf{x}, \mathbf{y}_i, \mathbf{u}) \end{aligned} \tag{53}$$

Here, use has been made of (49) and, on the right-hand side, the equality of mixed partials. Similarly, (52) and (50c) yield

$$\partial_{\mathbf{x}}C(\mathbf{x}, \mathbf{y}_i, \mathbf{u})\boldsymbol{\xi}_{\mathcal{P}}(\mathbf{x}) + \partial_{\mathbf{y}_i}C(\mathbf{x}, \mathbf{y}_i, \mathbf{u}) \left.\frac{\mathrm{d}}{\mathrm{d}s}\right|_{s=0} \mathbf{y}_i^s + \partial_{\mathbf{u}}C(\mathbf{x}, \mathbf{y}_i, \mathbf{u}) \left.\frac{\mathrm{d}}{\mathrm{d}s}\right|_{s=0} \mathbf{u}^s = \mathbf{0} \tag{54a}$$

$$\partial_{\mathbf{x}}\widetilde{\mathbf{g}}_i(\mathbf{x}, \mathbf{y}_i, \mathbf{u})\boldsymbol{\xi}_{\mathcal{P}}(\mathbf{x}) + \partial_{\mathbf{y}_i}\widetilde{\mathbf{g}}_i(\mathbf{x}, \mathbf{y}_i, \mathbf{u}) \left.\frac{\mathrm{d}}{\mathrm{d}s}\right|_{s=0} \mathbf{y}_i^s + \partial_{\mathbf{u}}\widetilde{\mathbf{g}}_i(\mathbf{x}, \mathbf{y}_i, \mathbf{u}) \left.\frac{\mathrm{d}}{\mathrm{d}s}\right|_{s=0} \mathbf{u}^s = \mathbf{0} \tag{54b}$$

Making use of the Hamiltonian (26), the optimality conditions (29) can be written in the form

$$\mathbf{0} = \boldsymbol{\lambda}^T\partial_{\mathbf{u}}\mathbf{f}_i(\mathbf{x}, \mathbf{y}_i, \mathbf{u}) + \boldsymbol{\eta}_i^T\partial_{\mathbf{u}}\widetilde{\mathbf{g}}_i(\mathbf{x}, \mathbf{y}_i, \mathbf{u}) - \partial_{\mathbf{u}}C(\mathbf{x}, \mathbf{y}_i, \mathbf{u}) \tag{55a}$$

$$\dot{\boldsymbol{\lambda}}^T = -\boldsymbol{\lambda}^T\partial_{\mathbf{x}}\mathbf{f}_i(\mathbf{x}, \mathbf{y}_i, \mathbf{u}) - \boldsymbol{\eta}_i^T\partial_{\mathbf{x}}\widetilde{\mathbf{g}}_i(\mathbf{x}, \mathbf{y}_i, \mathbf{u}) + \partial_{\mathbf{x}}C(\mathbf{x}, \mathbf{y}_i, \mathbf{u}) \tag{55b}$$

$$\mathbf{0} = \boldsymbol{\lambda}^T\partial_{\mathbf{y}_i}\mathbf{f}_i(\mathbf{x}, \mathbf{y}_i, \mathbf{u}) + \boldsymbol{\eta}_i^T\partial_{\mathbf{y}_i}\widetilde{\mathbf{g}}_i(\mathbf{x}, \mathbf{y}_i, \mathbf{u}) - \partial_{\mathbf{y}_i}C(\mathbf{x}, \mathbf{y}_i, \mathbf{u}) \tag{55c}$$

Multiplying (53) from the left by $\boldsymbol{\lambda}^T$ leads to

$$\begin{aligned} \boldsymbol{\lambda}^T\partial_{\mathbf{x}}\mathbf{f}_i(\mathbf{x}, \mathbf{y}_i, \mathbf{u})\boldsymbol{\xi}_{\mathcal{P}}(\mathbf{x}) \quad &+ \quad \boldsymbol{\lambda}^T\partial_{\mathbf{y}_i}\mathbf{f}_i(\mathbf{x}, \mathbf{y}_i, \mathbf{u}) \left.\frac{\mathrm{d}}{\mathrm{d}s}\right|_{s=0} \mathbf{y}_i^s \\ &+ \quad \boldsymbol{\lambda}^T\partial_{\mathbf{u}}\mathbf{f}_i(\mathbf{x}, \mathbf{y}_i, \mathbf{u}) \left.\frac{\mathrm{d}}{\mathrm{d}s}\right|_{s=0} \mathbf{u}^s = \boldsymbol{\lambda}^T D\boldsymbol{\xi}_{\mathcal{P}}(\mathbf{x})\mathbf{f}_i(\mathbf{x}, \mathbf{y}_i, \mathbf{u}) \end{aligned}$$

Substituting from (55a), (55b) and (55c) into the last equation yields

$$\begin{aligned} \boldsymbol{\lambda}^T D\boldsymbol{\xi}_{\mathcal{P}}(\mathbf{x})\mathbf{f}_i(\mathbf{x}, \mathbf{y}_i, \mathbf{u}) = \quad &- \left(\boldsymbol{\eta}_i^T\partial_{\mathbf{x}}\widetilde{\mathbf{g}}_i(\mathbf{x}, \mathbf{y}_i, \mathbf{u}) - \partial_{\mathbf{x}}C(\mathbf{x}, \mathbf{y}_i, \mathbf{u}) + \dot{\boldsymbol{\lambda}}^T\right)\boldsymbol{\xi}_{\mathcal{P}}(\mathbf{x}) \\ &- \left(\boldsymbol{\eta}_i^T\partial_{\mathbf{y}_i}\widetilde{\mathbf{g}}_i(\mathbf{x}, \mathbf{y}_i, \mathbf{u}) - \partial_{\mathbf{y}_i}C(\mathbf{x}, \mathbf{y}_i, \mathbf{u})\right) \left.\frac{\mathrm{d}}{\mathrm{d}s}\right|_{s=0} \mathbf{y}_i^s \\ &- \left(\boldsymbol{\eta}_i^T\partial_{\mathbf{u}}\widetilde{\mathbf{g}}_i(\mathbf{x}, \mathbf{y}_i, \mathbf{u}) - \partial_{\mathbf{u}}C(\mathbf{x}, \mathbf{y}_i, \mathbf{u})\right) \left.\frac{\mathrm{d}}{\mathrm{d}s}\right|_{s=0} \mathbf{u}^s \end{aligned}$$

Taking into account (54a) and (54b), the last equation can be recast in the form

$$\mathbf{0} = \dot{\boldsymbol{\lambda}}^T\boldsymbol{\xi}_{\mathcal{P}}(\mathbf{x}) + \boldsymbol{\lambda}^T D\boldsymbol{\xi}_{\mathcal{P}}(\mathbf{x})\mathbf{f}_i(\mathbf{x}, \mathbf{y}_i, \mathbf{u})$$

Inserting the state Eq. (22a) in the above equation yields

$$\mathbf{0} = \dot{\lambda}^T \boldsymbol{\xi}_{\mathcal{P}}(\mathbf{x}) + \lambda^T D\boldsymbol{\xi}_{\mathcal{P}}(\mathbf{x})\dot{\mathbf{x}} = \frac{d}{dt}\left(\lambda^T \boldsymbol{\xi}_{\mathcal{P}}(\mathbf{x})\right) \tag{56}$$

which confirms that quantity (51) is indeed conserved along optimal trajectories.

#### 4.1.2. Optimal control formulation according to the common approach

We next consider the optimal control formulation dealt with in Section 3.2. To this end, we directly start from the infinitesimal versions of the symmetry conditions (50), which are again given by (53) and (54a), together with the infinitesimal version of (50b) given by

$$\mathrm{D}\mathbf{g}_i(\mathbf{x})\boldsymbol{\xi}_{\mathcal{P}}(\mathbf{x}) = \mathbf{0} \tag{57}$$

Employing the Hamiltonian (30) in the optimality conditions (29) yields

$$\mathbf{0} = \lambda^T \partial_{\mathbf{u}} \mathbf{f}_i(\mathbf{x}, \mathbf{y}_i, \mathbf{u}) - \partial_{\mathbf{u}} C(\mathbf{x}, \mathbf{y}_i, \mathbf{u}) \tag{58a}$$

$$\dot{\lambda}^T = -\lambda^T \partial_{\mathbf{x}} \mathbf{f}_i(\mathbf{x}, \mathbf{y}_i, \mathbf{u}) - \boldsymbol{\eta}_i^T D\mathbf{g}_i(\mathbf{x}) + \partial_{\mathbf{x}} C(\mathbf{x}, \mathbf{y}_i, \mathbf{u}) \tag{58b}$$

$$\mathbf{0} = \lambda^T \partial_{\mathbf{y}_i} \mathbf{f}_i(\mathbf{x}, \mathbf{y}_i, \mathbf{u}) - \partial_{\mathbf{y}_i} C(\mathbf{x}, \mathbf{y}_i, \mathbf{u}) \tag{58c}$$

Multiplying (53) from the left by $\lambda^T$ leads to

$$\begin{aligned} \lambda^T \partial_{\mathbf{x}} \mathbf{f}_i(\mathbf{x}, \mathbf{y}_i, \mathbf{u}) \boldsymbol{\xi}_{\mathcal{P}}(\mathbf{x}) \quad &+ \quad \lambda^T \partial_{\mathbf{y}_i} \mathbf{f}_i(\mathbf{x}, \mathbf{y}_i, \mathbf{u}) \left.\frac{\mathrm{d}}{\mathrm{d}s}\right|_{s=0} \mathbf{y}_i^s \\ &+ \quad \lambda^T \partial_{\mathbf{u}} \mathbf{f}_i(\mathbf{x}, \mathbf{y}_i, \mathbf{u}) \left.\frac{\mathrm{d}}{\mathrm{d}s}\right|_{s=0} \mathbf{u}^s = \lambda^T D\boldsymbol{\xi}_{\mathcal{P}}(\mathbf{x}) \mathbf{f}_i(\mathbf{x}, \mathbf{y}_i, \mathbf{u}) \end{aligned}$$

Substituting from (58a), (58b) and (58c) into the last equation yields

$$\begin{aligned} \lambda^T D\boldsymbol{\xi}_{\mathcal{P}}(\mathbf{x}) \mathbf{f}_i(\mathbf{x}, \mathbf{y}_i, \mathbf{u}) = \quad & \left(\partial_{\mathbf{x}} C(\mathbf{x}, \mathbf{y}_i, \mathbf{u}) - \boldsymbol{\eta}_i^T D\mathbf{g}_i(\mathbf{x}) - \dot{\lambda}^T\right) \boldsymbol{\xi}_{\mathcal{P}}(\mathbf{x}) \\ &+ \partial_{\mathbf{y}_i} C(\mathbf{x}, \mathbf{y}_i, \mathbf{u}) \left.\frac{\mathrm{d}}{\mathrm{d}s}\right|_{s=0} \mathbf{y}_i^s \\ &+ \partial_{\mathbf{u}} C(\mathbf{x}, \mathbf{y}_i, \mathbf{u}) \left.\frac{\mathrm{d}}{\mathrm{d}s}\right|_{s=0} \mathbf{u}^s \end{aligned}$$

Substituting (57) and (54a) into the last equation yields

$$\mathbf{0} = \dot{\lambda}^T \boldsymbol{\xi}_{\mathcal{P}}(\mathbf{x}) + \lambda^T D\boldsymbol{\xi}_{\mathcal{P}}(\mathbf{x}) \mathbf{f}_i(\mathbf{x}, \mathbf{y}_i, \mathbf{u})$$

from which again follows result (56).

### 4.2. Conservation of optimal control Hamiltonians

Next, we verify that both optimal control formulations considered in this work conserve the optimal control Hamiltonian.

#### 4.2.1. Optimal control formulation based on the maximum principle

The optimal control Hamiltonian (26) is a conserved quantity of the optimal control formulation based on the maximum principle (Section 3.1). To see this, differentiate (26) with respect to time to obtain

$$\begin{aligned} \tfrac{d}{dt}\mathcal{H}_i(\mathbf{x}, \mathbf{y}_i, \mathbf{u}, \lambda, \boldsymbol{\eta}_i) \quad &= \partial_{\mathbf{x}} \mathcal{H}_i \dot{\mathbf{x}} + \partial_{\mathbf{y}_i} \mathcal{H}_i \dot{\mathbf{y}}_i + \partial_{\mathbf{u}} \mathcal{H}_i \dot{\mathbf{u}} + \partial_{\lambda} \mathcal{H}_i \dot{\lambda} + \partial_{\boldsymbol{\eta}_i} \mathcal{H}_i \dot{\boldsymbol{\eta}}_i \\ &= \partial_{\mathbf{x}} \mathcal{H}_i \nabla_{\lambda} \mathcal{H}_i + \partial_{\lambda} \mathcal{H}_i \left(-\nabla_{\mathbf{x}} \mathcal{H}_i\right) + \widetilde{\mathbf{g}}_i^T \dot{\boldsymbol{\eta}}_i \\ &= \widetilde{\mathbf{g}}_i^T \dot{\boldsymbol{\eta}}_i \end{aligned}$$

where the optimality conditions (29) have been used. Now, for $i = 2$, expression (28) leads to

$$\widetilde{\mathbf{g}}_2 = D\mathbf{g}_2(\mathbf{x})\mathbf{f}_2 = D\mathbf{g}_2(\mathbf{x})\dot{\mathbf{x}} = \frac{d}{dt}\mathbf{g}_2(\mathbf{x}) = \mathbf{0}$$

which follows from the fulfillment of the constraints $\mathbf{g}_2(\mathbf{x}) = \mathbf{0}$. Similarly, for $i = 3$, relation (27) yields

$$\widetilde{\mathbf{g}}_3 = D\mathbf{g}^v(\mathbf{x})\mathbf{f}_3 = D\mathbf{g}^v(\mathbf{x})\dot{\mathbf{x}} = \frac{d}{dt}\mathbf{g}^v(\mathbf{x}) = \frac{d^2}{dt^2}\mathbf{g}^q(\mathbf{q}) = \mathbf{0}$$

which follows from the fulfillment of the constraints $\mathbf{g}^q(\mathbf{q}) = \mathbf{0}$. Thus, we obtain the result

$$\frac{d}{dt}\mathcal{H}_i = 0$$

so that $\mathcal{H}_i$ is conserved along optimal trajectories for $i \in \{2, 3\}$.

*4.2.2. Optimal control formulation according to the common approach*

We now turn to the Hamiltonian (30) associated with the common approach (Section 3.2). Differentiating (30) with respect to time yields

$$\begin{aligned}\frac{d}{dt}\overline{\mathcal{H}}_i(\mathbf{x},\mathbf{y}_i,\mathbf{u},\lambda,\boldsymbol{\eta}_i) &= \partial_{\mathbf{x}}\overline{\mathcal{H}}_i\dot{\mathbf{x}} + \partial_{\mathbf{y}_i}\overline{\mathcal{H}}_i\dot{\mathbf{y}}_i + \partial_{\mathbf{u}}\overline{\mathcal{H}}_i\dot{\mathbf{u}} + \partial_{\lambda}\overline{\mathcal{H}}_i\dot{\lambda} + \partial_{\boldsymbol{\eta}_i}\overline{\mathcal{H}}_i\dot{\boldsymbol{\eta}}_i \\ &= \partial_{\mathbf{x}}\overline{\mathcal{H}}_i\nabla_{\lambda}\overline{\mathcal{H}}_i + \partial_{\lambda}\overline{\mathcal{H}}_i\left(-\nabla_{\mathbf{x}}\overline{\mathcal{H}}_i\right) \\ &= \mathbf{0}\end{aligned}$$

Here, use has been made of the optimality conditions (29) and (31) (in terms of $\overline{\mathcal{H}}_i$). Accordingly, $\overline{\mathcal{H}}_i$ is a conserved quantity of the optimal control problem for $i \in \{2,3\}$.

## 5. Structure-preserving discretization

In this section we devise a direct discretization approach that yields structure-preserving discrete conditions of optimality. In particular, the resulting schemes inherit the conservation of generalized momentum maps from the underlying continuous optimal control problem with symmetry. Our approach can be viewed as generalization of the direct method [27], that is confined to state equations in ODE form.

We start with generic functions $\mathbf{f}_d(\mathbf{x},\mathbf{y},\mathbf{u})$, $\mathbf{g}_d(\mathbf{x},\mathbf{y},\mathbf{u})$, and $C_d(\mathbf{x},\mathbf{y},\mathbf{u})$, which in the sequel shall be adopted to specific forms of, respectively, the state equations, the constraint functions and the density cost function. Let the time interval of interest, $I \in [t_0,t_f]$, be split in $N$ non-overlapping subintervals $I_n = [t_n,t_{n+1}] = [nh,(n+1)h]$ $(n = 0,1,\dots,N-1)$ of length $h = \frac{t_f-t_0}{N}$. The discrete value of a function $\mathbf{f} : I \to \mathbb{R}^d$ at time $t_n$ is denoted by $\mathbf{f}_n$. To approximate augmented cost functionals such as (32), we introduce a discrete augmented cost function of the form

$$\begin{aligned}S_d = \sum_{n=0}^{N-1}\Big[&\lambda_{n+1}^T\big(\mathbf{x}_{n+1}-\mathbf{x}_n-\mathbf{f}_d\big((1-\alpha)\mathbf{x}_n+\alpha\mathbf{a}_n,\mathbf{y}_{n+1},\mathbf{u}_{n+1}\big)\big)\\ &+\boldsymbol{\alpha}_n^T\big(\mathbf{a}_n-\mathbf{x}_n-\mathbf{f}_d\big((1-\alpha)\mathbf{x}_n+\alpha\mathbf{a}_n,\mathbf{y}_{n+1},\mathbf{u}_{n+1}\big)\big)\\ &-\boldsymbol{\eta}_{n+1}^T\mathbf{g}_d\big((1-\alpha)\mathbf{x}_n+\alpha\mathbf{a}_n,\mathbf{y}_{n+1},\mathbf{u}_{n+1}\big)\\ &+C_d\big((1-\alpha)\mathbf{x}_n+\alpha\mathbf{a}_n,\mathbf{y}_{n+1},\mathbf{u}_{n+1}\big)\Big]\\ &+\lambda_0^T(\mathbf{x}_0-\bar{\mathbf{x}}_0)+\boldsymbol{\gamma}^T\mathbf{g}_f(\mathbf{x}_N)\end{aligned} \tag{59}$$

where $\alpha \in [0,1]$. Note that $S_d$ depends on the discrete state variables $\mathbf{x}_n$ $(n = 0,\dots,N)$, auxiliary state variables $\mathbf{a}_n$ $(n = 0,\dots,N-1)$, discrete mechanical multipliers $\mathbf{y}_n$ $(n = 1,\dots,N)$, discrete controls $\mathbf{u}_n$ $(n = 1,\dots,N)$, and discrete Lagrange multipliers $\lambda_n$ $(n = 0,\dots,N)$, $\boldsymbol{\alpha}_n$, $(n = 0,\dots,N-1)$, $\boldsymbol{\eta}_n$ $(n = 1,\dots,N)$, and $\boldsymbol{\gamma} \in \mathbf{R}^{2n_{\text{dof}}}$. The multipliers $\boldsymbol{\gamma}$ are used to enforce the final state constraints

$$\mathbf{g}_f(\mathbf{x}_N) = \mathbf{0} \tag{60}$$

Imposing the stationary conditions on $S_d$ yields the discrete Euler–Lagrange equations. In particular, stationary with respect to the Lagrange multipliers $\lambda_n$ and $\boldsymbol{\alpha}_n$ yields

$$\mathbf{a}_n = \mathbf{x}_{n+1}$$

together with the discretized differential part of the state DAEs

$$\mathbf{x}_{n+1}-\mathbf{x}_n = \mathbf{f}_d(\mathbf{x}_{n+\alpha},\mathbf{y}_{n+1},\mathbf{u}_{n+1}) \tag{61}$$

where

$$\mathbf{x}_{n+\alpha} = (1-\alpha)\mathbf{x}_n + \alpha\mathbf{x}_{n+1} \tag{62}$$

Variation with respect to $\mathbf{x}_n$ and $\mathbf{a}_n$ yields

$$\boldsymbol{\alpha}_n = -\alpha(\lambda_{n+1}-\lambda_n) \tag{63}$$

together with

$$\begin{aligned}\lambda_{n+1}-\lambda_n = &-\partial_{\mathbf{x}}\mathbf{f}_d(\mathbf{x}_{n+\alpha},\mathbf{y}_{n+1},\mathbf{u}_{n+1})^T\lambda_{n+(1-\alpha)}\\ &-\partial_{\mathbf{x}}\mathbf{g}_d(\mathbf{x}_{n+\alpha},\mathbf{y}_{n+1},\mathbf{u}_{n+1})^T\boldsymbol{\eta}_{n+1}\\ &+\partial_{\mathbf{x}}C_d(\mathbf{x}_{n+\alpha},\mathbf{y}_{n+1},\mathbf{u}_{n+1})^T\end{aligned} \tag{64}$$

where

$$\lambda_{n+(1-\alpha)} = \alpha\lambda_n + (1-\alpha)\lambda_{n+1} \tag{65}$$

Note that (64) represents the discrete version of the differential part of the adjoint DAEs. The discrete counterpart of the algebraic part of the adjoint DAEs results from the stationary condition of $S_d$ with respect to $\mathbf{y}_n$ leading to

$$\begin{aligned}\mathbf{0} = &\partial_{\mathbf{y}}\mathbf{f}_d(\mathbf{x}_{n+\alpha},\mathbf{y}_{n+1},\mathbf{u}_{n+1})^T\lambda_{n+(1-\alpha)}\\ &\partial_{\mathbf{y}}\mathbf{g}_d(\mathbf{x}_{n+\alpha},\mathbf{y}_{n+1},\mathbf{u}_{n+1})^T\boldsymbol{\eta}_{n+1}\\ &-\partial_{\mathbf{y}}C_d(\mathbf{x}_{n+\alpha},\mathbf{y}_{n+1},\mathbf{u}_{n+1})^T\end{aligned} \tag{66}$$

Similarly, stationary with respect to $\mathbf{u}_n$ yields the discrete optimality conditions

$$\begin{aligned}\mathbf{0} =&\partial_{\mathbf{u}}\mathbf{f}_d(\mathbf{x}_{n+\alpha},\mathbf{y}_{n+1},\mathbf{u}_{n+1})^T\lambda_{n+(1-\alpha)}\\ &\partial_{\mathbf{u}}\mathbf{g}_d(\mathbf{x}_{n+\alpha},\mathbf{y}_{n+1},\mathbf{u}_{n+1})^T\boldsymbol{\eta}_{n+1}\\ &-\partial_{\mathbf{u}}C_d(\mathbf{x}_{n+\alpha},\mathbf{y}_{n+1},\mathbf{u}_{n+1})^T\end{aligned} \tag{67}$$

Eventually, stationary with respect to the multipliers $\boldsymbol{\eta}_n$ gives

$$\mathbf{g}_d(\mathbf{x}_{n+\alpha},\mathbf{y}_{n+1},\mathbf{u}_{n+1}) = \mathbf{0} \tag{68}$$

The above discrete conditions of optimality can be written in compact form by introducing the discrete optimal control Hamiltonian

$$\mathcal{H}_d(\mathbf{x},\mathbf{y},\mathbf{u},\lambda,\boldsymbol{\eta}) = \lambda^T\mathbf{f}_d(\mathbf{x},\mathbf{y},\mathbf{u}) + \boldsymbol{\eta}^T\mathbf{g}_d(\mathbf{x},\mathbf{y},\mathbf{u}) - C_d(\mathbf{x},\mathbf{y},\mathbf{u}) \tag{69}$$

to obtain

$$\mathbf{x}_{n+1} - \mathbf{x}_n = \quad \nabla_\lambda\mathcal{H}_d(\mathbf{x}_{n+\alpha},\mathbf{y}_{n+1},\mathbf{u}_{n+1},\lambda_{n+(1-\alpha)},\boldsymbol{\eta}_{n+1}) \tag{70a}$$

$$\mathbf{0} = \quad \nabla_{\boldsymbol{\eta}}\mathcal{H}_d(\mathbf{x}_{n+\alpha},\mathbf{y}_{n+1},\mathbf{u}_{n+1},\lambda_{n+(1-\alpha)},\boldsymbol{\eta}_{n+1}) \tag{70b}$$

$$\lambda_{n+1} - \lambda_n = -\nabla_{\mathbf{x}}\mathcal{H}_d(\mathbf{x}_{n+\alpha},\mathbf{y}_{n+1},\mathbf{u}_{n+1},\lambda_{n+(1-\alpha)},\boldsymbol{\eta}_{n+1}) \tag{70c}$$

$$\mathbf{0} = \quad \nabla_{\mathbf{y}}\mathcal{H}_d(\mathbf{x}_{n+\alpha},\mathbf{y}_{n+1},\mathbf{u}_{n+1},\lambda_{n+(1-\alpha)},\boldsymbol{\eta}_{n+1}) \tag{70d}$$

$$\mathbf{0} = \quad \nabla_{\mathbf{u}}\mathcal{H}_d(\mathbf{x}_{n+\alpha},\mathbf{y}_{n+1},\mathbf{u}_{n+1},\lambda_{n+(1-\alpha)},\boldsymbol{\eta}_{n+1}) \tag{70e}$$

for $\alpha \in (0,1]$ and $n = 0,\dots,N-1$. Furthermore, we get the boundary and transversality conditions

$$\mathbf{0} = \mathbf{x}_0 - \bar{\mathbf{x}}_0 \tag{71a}$$

$$\mathbf{0} = \mathbf{g}_f(\mathbf{x}_N) \tag{71b}$$

$$\mathbf{0} = \lambda_N + D\mathbf{g}_f(\mathbf{x}_N)^T\boldsymbol{\gamma} \tag{71c}$$

Note that the specific form (60) of the final state constraints accounts for the fact that the constraints are enforced in each time step through (70b) including the final one at $n = N-1$.

### 5.1. Direct method based on the common approach

The direct discretization approach developed above can be directly applied to the optimal control formulation based on the common approach (Section 3.2). To this end, we choose

$$\mathbf{f}_d(\mathbf{x},\mathbf{y},\mathbf{u}) = h\mathbf{f}_i(\mathbf{x},\mathbf{y}_i,\mathbf{u}) \tag{72a}$$

$$\mathbf{g}_d(\mathbf{x},\mathbf{y},\mathbf{u}) = h\mathbf{g}_i(\mathbf{x}) \tag{72b}$$

$$C_d(\mathbf{x},\mathbf{y},\mathbf{u}) = hC(\mathbf{x},\mathbf{y}_i,\mathbf{u}) \tag{72c}$$

This choice implies that the discrete Hamiltonian (69), $\mathcal{H}_d = h\overline{\mathcal{H}}_i$ ($i \in \{2,3\}$), where Hamiltonian $\overline{\mathcal{H}}_i$ has been introduced in (30). Correspondingly, the discrete conditions of optimality in (70) can now be recast in the form

$$\mathbf{x}_{n+1} - \mathbf{x}_n = \quad h\nabla_\lambda\overline{\mathcal{H}}_i(\mathbf{x}_{n+\alpha},\mathbf{y}_{n+1},\mathbf{y}_{i_{n+1}},\lambda_{n+(1-\alpha)},\boldsymbol{\eta}_{i_{n+1}}) \tag{73a}$$

$$\mathbf{0} = \quad \nabla_{\boldsymbol{\eta}_i}\overline{\mathcal{H}}_i(\mathbf{x}_{n+\alpha},\mathbf{y}_{i_{n+1}},\mathbf{u}_{n+1},\lambda_{n+(1-\alpha)},\boldsymbol{\eta}_{i_{n+1}}) \tag{73b}$$

$$\lambda_{n+1} - \lambda_n = -h\nabla_{\mathbf{x}}\overline{\mathcal{H}}_i(\mathbf{x}_{n+\alpha},\mathbf{y}_{i_{n+1}},\mathbf{u}_{n+1},\lambda_{n+(1-\alpha)},\boldsymbol{\eta}_{i_{n+1}}) \tag{73c}$$

$$\mathbf{0} = \quad \nabla_{\mathbf{y}}\overline{\mathcal{H}}_i(\mathbf{x}_{n+\alpha},\mathbf{y}_{i_{n+1}},\mathbf{u}_{n+1},\lambda_{n+(1-\alpha)},\boldsymbol{\eta}_{i_{n+1}}) \tag{73d}$$

$$\mathbf{0} = \quad \nabla_{\mathbf{u}}\overline{\mathcal{H}}_i(\mathbf{x}_{n+\alpha},\mathbf{y}_{i_{n+1}},\mathbf{u}_{n+1},\lambda_{n+(1-\alpha)},\boldsymbol{\eta}_{i_{n+1}}) \tag{73e}$$

Note that (73b) yields $\mathbf{g}_i(\mathbf{x}_{n+\alpha}) = \mathbf{0}$. Obviously, the above scheme can also be obtained by directly discretizing the continuous optimality conditions dealt with in Section 3.2. Accordingly, the direct and the indirect approach commute.

### 5.2. Numerical methods based on the maximum principle

As has been outlined in Remark 1, the structural discrepancy of the optimal control formulation based on the maximum principle impairs the design of direct methods. In what follows, we first propose an indirect method which relies on a slight modification of the above-developed direct method. We then show that, under certain conditions, the direct approach can be maintained by making slight adjustments to the above-developed direct method.

#### 5.2.1. Indirect method

To take into account the structural discrepancy of the optimal control formulation based on the maximum principle, we propose an indirect method which can be obtained by modifying the above-developed direct method. Accordingly, we choose

$$\mathbf{f}_d(\mathbf{x},\mathbf{y},\mathbf{u}) = h\mathbf{f}_i(\mathbf{x},\mathbf{y}_i,\mathbf{u}) \tag{74a}$$

$$\mathbf{g}_d(\mathbf{x},\mathbf{y},\mathbf{u}) = h\widetilde{\mathbf{g}}_i(\mathbf{x},\mathbf{y}_i,\mathbf{u}) \tag{74b}$$

$$C_d(\mathbf{x},\mathbf{y},\mathbf{u}) = hC(\mathbf{x},\mathbf{y}_i,\mathbf{u}) \tag{74c}$$

and define

$$\mathbf{x}_{n+1} - \mathbf{x}_n = \quad h\mathbf{f}_i(\mathbf{x}_{n+\alpha},\mathbf{y}_{i_{n+1}},\boldsymbol{\eta}_{i_{n+1}}) \tag{75a}$$

$$\mathbf{0} = \quad \mathbf{g}_i(\mathbf{x}_{n+1}) \tag{75b}$$

$$\lambda_{n+1} - \lambda_n = -h\nabla_{\mathbf{x}}\mathcal{H}_i(\mathbf{x}_{n+\alpha},\mathbf{y}_{i_{n+1}},\mathbf{u}_{n+1},\lambda_{n+(1-\alpha)},\boldsymbol{\eta}_{i_{n+1}}) \tag{75c}$$

$$\mathbf{0} = \quad \nabla_{\mathbf{y}}\mathcal{H}_i(\mathbf{x}_{n+\alpha},\mathbf{y}_{i_{n+1}},\mathbf{u}_{n+1},\lambda_{n+(1-\alpha)},\boldsymbol{\eta}_{i_{n+1}}) \tag{75d}$$

$$\mathbf{0} = \quad \nabla_{\mathbf{u}}(\mathbf{x}_{n+\alpha},\mathbf{y}_{n+1},\mathbf{y}_{i_{n+1}},\lambda_{n+(1-\alpha)},\boldsymbol{\eta}_{i_{n+1}}) \tag{75e}$$

Note that the choice (74) renders the discrete Hamiltonian (69) to be equal to $\mathcal{H}_d = h\mathcal{H}_i$, where Hamiltonian $\mathcal{H}_i$ has been introduced in (26). Furthermore, concerning the algebraic constraints in (75b),

$$\mathbf{g}_i(\mathbf{x}_{n+1}) \neq \nabla_{\boldsymbol{\eta}_i}\mathcal{H}_i(\mathbf{x}_{n+\alpha},\mathbf{y}_{i_{n+1}},\mathbf{u}_{n+1},\lambda_{n+(1-\alpha)},\boldsymbol{\eta}_{i_{n+1}})$$

which is in line with the structural discrepancy outlined in Remark 1. Moreover, (75b) ensures that the mechanical constraints are satisfied at the discrete time nodes, independent of the choice for $\alpha \in [0,1]$.

Scheme (75) can be obtained by directly discretizing the continuous state equations in (25), along with the conditions of optimality (29), and thus follows from the indirect approach characterized by "first optimize then discretize".

#### 5.2.2. Direct method due to Martens & Gerdts [20]

Despite the structural discrepancy outlined in Remark 1, it is possible to apply the direct approach developed above in a consistent way to the optimal control formulation based on the maximum principle. For $i = 2$ and $\alpha = 1$ this was shown recently in [20]. The main idea is to write $\widetilde{\mathbf{g}}_2(\mathbf{x},\mathbf{y}_2,\mathbf{u})$, introduced in (28), as $\widetilde{\mathbf{g}}_2 = d\mathbf{g}_2(\mathbf{x})/dt$ and apply the difference quotient to obtain the discrete version

$$\widetilde{\mathbf{g}}_d = \frac{1}{h}\left(\mathbf{g}_2(\mathbf{x}_{n+1}) - \mathbf{g}_2(\mathbf{x}_n)\right) \tag{76}$$

Now, choosing again $\mathbf{f}_d(\mathbf{x},\mathbf{y},\mathbf{u}) = h\mathbf{f}_i(\mathbf{x},\mathbf{y}_i,\mathbf{u})$, together with $i = 2$ and $\alpha = 1$, the discrete state Eq. (61) can be written in the form

$$\mathbf{x}_n = \mathbf{x}_{n+1} - h\mathbf{f}_2(\mathbf{x}_{n+1},\mathbf{y}_{2_{n+1}},\mathbf{u}_{n+1})$$

Inserting the last equation into (76) yields

$$\widetilde{\mathbf{g}}_d^{(1)}(\mathbf{x}_{n+1},\mathbf{y}_{2_{n+1}},\mathbf{u}_{n+1}) = \frac{1}{h}\left(\mathbf{g}_2(\mathbf{x}_{n+1}) + \mathbf{g}_2\big(\mathbf{x}_{n+1} - h\mathbf{f}_2(\mathbf{x}_{n+1},\mathbf{y}_{2_{n+1}},\mathbf{u}_{n+1})\big)\right) \tag{77}$$

Formula (77) represents a viable discretization of $\widetilde{\mathbf{g}}_2(\mathbf{x},\mathbf{y}_2,\mathbf{u})$. To summarize, we choose

$$\mathbf{f}_d(\mathbf{x},\mathbf{y},\mathbf{u}) = h\mathbf{f}_2(\mathbf{x},\mathbf{y}_2,\mathbf{u}) \tag{78a}$$

$$\mathbf{g}_d(\mathbf{x},\mathbf{y},\mathbf{u}) = h\widetilde{\mathbf{g}}_d^{(1)}(\mathbf{x},\mathbf{y}_2,\mathbf{u}) \tag{78b}$$

$$C_d(\mathbf{x},\mathbf{y},\mathbf{u}) = hC(\mathbf{x},\mathbf{y}_2,\mathbf{u}) \tag{78c}$$

in the discrete Hamiltonian (69). The resulting discrete conditions of optimality assume the form (70) with $\alpha = 1$. In particular, (70b) yields $\mathbf{g}_d(\mathbf{x}_{n+1},\mathbf{y}_{2_{n+1}},\mathbf{u}_{n+1}) = \mathbf{0}$, which implies $\mathbf{g}_2(\mathbf{x}_{n+1}) = \mathbf{0}$, provided that $\mathbf{g}_2(\mathbf{x}_n) = \mathbf{0}$ is satisfied.

#### 5.2.3. Direct method based on the discrete derivative

While the direct method in Section 5.2.2 is based on $\alpha = 1$, and thus confined to first-order accuracy, we next propose an alternative procedure which again fits into the framework of the direct approach developed above and allows for second-order accuracy. As in Section 5.2.2, we confine our attention to $i = 2$. Our approach is based on the notion of *discrete derivative* [31]. In particular, the directionality property of the discrete derivative implies

$$\mathbf{g}_2(\mathbf{x}_{n+1}) - \mathbf{g}_2(\mathbf{x}_n) = \mathrm{D}\mathbf{g}_2(\mathbf{x}_n,\mathbf{x}_{n+1})(\mathbf{x}_{n+1} - \mathbf{x}_n) \tag{79}$$

where $\mathrm{D}\mathbf{g}_2(\mathbf{x}_n,\mathbf{x}_{n+1})$ stands for the discrete derivative of $\mathbf{g}_2(\mathbf{x})$. If the constraints $\mathbf{g}_2(\mathbf{x})$ are at most quadratic functions, the discrete derivative coincides with the derivative evaluated in the mid-point, i.e. $\mathrm{D}\mathbf{g}_2(\mathbf{x}_n,\mathbf{x}_{n+1}) = D\mathbf{g}_2(\mathbf{x}_{n+\frac{1}{2}})$. This suggests to focus on $\alpha = 1/2$. Inserting (79) into (76) and choosing $\mathbf{f}_d(\mathbf{x},\mathbf{y},\mathbf{u}) = h\mathbf{f}_2(\mathbf{x},\mathbf{y}_2,\mathbf{u})$, we obtain

$$\widetilde{\mathbf{g}}_d^{(2)}(\mathbf{x}_{n+\frac{1}{2}},\mathbf{y}_{2_{n+1}},\mathbf{u}_{n+1}) = \frac{1}{h}D\mathbf{g}_2(\mathbf{x}_{n+\frac{1}{2}})\mathbf{f}_2(\mathbf{x}_{n+\frac{1}{2}},\mathbf{y}_{2_{n+1}},\mathbf{u}_{n+1}) \tag{80}$$

To summarize, we choose

$$\mathbf{f}_d(\mathbf{x},\mathbf{y},\mathbf{u}) = h\mathbf{f}_2(\mathbf{x},\mathbf{y}_2,\mathbf{u}) \tag{81a}$$

$$\mathbf{g}_d(\mathbf{x},\mathbf{y},\mathbf{u}) = h\widetilde{\mathbf{g}}_d^{(2)}(\mathbf{x},\mathbf{y}_2,\mathbf{u}) \tag{81b}$$

$$C_d(\mathbf{x},\mathbf{y},\mathbf{u}) = hC(\mathbf{x},\mathbf{y}_2,\mathbf{u}) \tag{81c}$$

in the discrete Hamiltonian (69). The resulting discrete conditions of optimality assume the form (70) with $\alpha = 1/2$. In particular, (70b) yields $\mathbf{g}_d(\mathbf{x}_{n+1},\mathbf{y}_{2_{n+1}},\mathbf{u}_{n+1}) = \mathbf{0}$, which again implies $\mathbf{g}_2(\mathbf{x}_{n+1}) = \mathbf{0}$, provided that $\mathbf{g}_2(\mathbf{x}_n) = \mathbf{0}$ is satisfied.

### 5.3. Discrete preservation of generalized momentum maps

We show that all of the schemes presented above are capable to conserve generalized momentum maps of the form (51). To this end, we assume that symmetry conditions (53), (54a) and (54a) hold and lead to the discrete counterparts

$$\begin{aligned}&\partial_{\mathbf{x}}\mathbf{f}_d(\mathbf{x}_{n+\alpha},\mathbf{y}_{n+1},\mathbf{u}_{n+1})\boldsymbol{\xi}_{\mathcal{P}}(\mathbf{x}_{n+\alpha}) + \partial_{\mathbf{y}}\mathbf{f}_d(\mathbf{x}_{n+\alpha},\mathbf{y}_{n+1},\mathbf{u}_{n+1})\left.\frac{\mathrm{d}}{\mathrm{d}s}\right|_{s=0}\mathbf{y}_{n+1}^s \\ &\quad + \partial_{\mathbf{u}}\mathbf{f}_d(\mathbf{x}_{n+\alpha},\mathbf{y}_{n+1},\mathbf{u}_{n+1})\left.\frac{\mathrm{d}}{\mathrm{d}s}\right|_{s=0}\mathbf{u}_{n+1}^s = D\boldsymbol{\xi}_{\mathcal{P}}(\mathbf{x}_{n+\alpha})\mathbf{f}_d(\mathbf{x}_{n+\alpha},\mathbf{y}_{n+1},\mathbf{u}_{n+1})\end{aligned} \tag{82}$$

$$\begin{aligned}&\partial_{\mathbf{x}}C_d(\mathbf{x}_{n+\alpha},\mathbf{y}_{n+1},\mathbf{u}_{n+1})\boldsymbol{\xi}_{\mathcal{P}}(\mathbf{x}_{n+\alpha}) + \partial_{\mathbf{y}}C_d(\mathbf{x}_{n+\alpha},\mathbf{y}_{n+1},\mathbf{u}_{n+1})\left.\frac{\mathrm{d}}{\mathrm{d}s}\right|_{s=0}\mathbf{y}_{n+1}^s \\ &\quad + \partial_{\mathbf{u}}C_d(\mathbf{x}_{n+\alpha},\mathbf{y}_{n+1},\mathbf{u}_{n+1})\left.\frac{\mathrm{d}}{\mathrm{d}s}\right|_{s=0}\mathbf{u}_{n+1}^s = \mathbf{0}\end{aligned} \tag{83}$$

$$\begin{aligned}&\partial_{\mathbf{x}}\mathbf{g}_d(\mathbf{x}_{n+\alpha},\mathbf{y}_{n+1},\mathbf{u}_{n+1})\boldsymbol{\xi}_{\mathcal{P}}(\mathbf{x}_{n+\alpha}) + \partial_{\mathbf{y}}\mathbf{g}_d(\mathbf{x}_{n+\alpha},\mathbf{y}_{n+1},\mathbf{u}_{n+1})\left.\frac{\mathrm{d}}{\mathrm{d}s}\right|_{s=0}\mathbf{y}_{n+1}^s \\ &\quad + \partial_{\mathbf{u}}\mathbf{g}_d(\mathbf{x}_{n+\alpha},\mathbf{y}_{n+1},\mathbf{u}_{n+1})\left.\frac{\mathrm{d}}{\mathrm{d}s}\right|_{s=0}\mathbf{u}_{n+1}^s = \mathbf{0}\end{aligned} \tag{84}$$

It can be shown by a straightforward calculation that the following identity holds:

$$\begin{aligned}J_{\xi_{n+1}} - J_{\xi_n} &= \boldsymbol{\lambda}_{n+1}^T\boldsymbol{\xi}_{\mathcal{P}}(\mathbf{x}_{n+1}) - \boldsymbol{\lambda}_n^T\boldsymbol{\xi}_{\mathcal{P}}(\mathbf{x}_n) \\ &= \left(\boldsymbol{\lambda}_{n+1}^T - \boldsymbol{\lambda}_n^T\right)\boldsymbol{\xi}_{\mathcal{P}}(\mathbf{x}_{n+\alpha}) + \boldsymbol{\lambda}_{n+(1-\alpha)}^T\boldsymbol{\xi}_{\mathcal{P}}(\mathbf{x}_{n+1} - \mathbf{x}_n)\end{aligned}$$

Here, it has been taken into account that $\boldsymbol{\xi}_{\mathcal{P}}(\mathbf{x})$ is at most linear in $\mathbf{x}$. Substituting (64) into the last equation yields

$$\begin{aligned}J_{\xi_{n+1}} - J_{\xi_n} =& -\boldsymbol{\lambda}_{n+(1-\alpha)}^T\partial_{\mathbf{x}}\mathbf{f}_d(\mathbf{x}_{n+\alpha},\mathbf{y}_{n+1},\mathbf{u}_{n+1})\boldsymbol{\xi}_{\mathcal{P}}(\mathbf{x}_{n+\alpha}) \\ &- \boldsymbol{\eta}_{n+1}^T\partial_{\mathbf{x}}\mathbf{g}_d(\mathbf{x}_{n+\alpha},\mathbf{y}_{n+1},\mathbf{u}_{n+1})\boldsymbol{\xi}_{\mathcal{P}}(\mathbf{x}_{n+\alpha}) \\ &+ \partial_{\mathbf{x}}C_d(\mathbf{x}_{n+\alpha},\mathbf{y}_{n+1},\mathbf{u}_{n+1})\boldsymbol{\xi}_{\mathcal{P}}(\mathbf{x}_{n+\alpha}) \\ &+ \boldsymbol{\lambda}_{n+(1-\alpha)}^T\boldsymbol{\xi}_{\mathcal{P}}(\mathbf{x}_{n+1} - \mathbf{x}_n)\end{aligned}$$

Making use of (84), (82) together with (61), the last equation can be recast in the form

$$\begin{aligned}J_{\xi_{n+1}} - J_{\xi_n} =& \left(\boldsymbol{\lambda}_{n+(1-\alpha)}^T\partial_{\mathbf{y}}\mathbf{f}_d(\mathbf{x}_{n+\alpha},\mathbf{y}_{n+1},\mathbf{u}_{n+1}) + \boldsymbol{\eta}_{n+1}^T\partial_{\mathbf{y}}\mathbf{g}_d(\mathbf{x}_{n+\alpha},\mathbf{y}_{n+1},\mathbf{u}_{n+1})\right)\left.\frac{\mathrm{d}}{\mathrm{d}s}\right|_{s=0}\mathbf{y}_{n+1}^s \\ &+ \left(\boldsymbol{\lambda}_{n+(1-\alpha)}^T\partial_{\mathbf{u}}\mathbf{f}_d(\mathbf{x}_{n+\alpha},\mathbf{y}_{n+1},\mathbf{u}_{n+1}) + \boldsymbol{\eta}_{n+1}^T\partial_{\mathbf{u}}\mathbf{g}_d(\mathbf{x}_{n+\alpha},\mathbf{y}_{n+1},\mathbf{u}_{n+1})\right)\left.\frac{\mathrm{d}}{\mathrm{d}s}\right|_{s=0}\mathbf{u}_{n+1}^s \\ &+ \partial_{\mathbf{x}}C_d(\mathbf{x}_{n+\alpha},\mathbf{y}_{n+1},\mathbf{u}_{n+1})\boldsymbol{\xi}_{\mathcal{P}}(\mathbf{x}_{n+\alpha})\end{aligned}$$

Substituting from (66) and (67) into the last equation yields

$$\begin{aligned}J_{\xi_{n+1}} - J_{\xi_n} =& \partial_{\mathbf{y}}C_d(\mathbf{x}_{n+\alpha},\mathbf{y}_{n+1},\mathbf{u}_{n+1})\left.\frac{\mathrm{d}}{\mathrm{d}s}\right|_{s=0}\mathbf{y}_{n+1}^s + \partial_{\mathbf{u}}C_d(\mathbf{x}_{n+\alpha},\mathbf{y}_{n+1},\mathbf{u}_{n+1})\left.\frac{\mathrm{d}}{\mathrm{d}s}\right|_{s=0}\mathbf{u}_{n+1}^s \\ &+ \partial_{\mathbf{x}}C_d(\mathbf{x}_{n+\alpha},\mathbf{y}_{n+1},\mathbf{u}_{n+1})\boldsymbol{\xi}_{\mathcal{P}}(\mathbf{x}_{n+\alpha})\end{aligned}$$

Inserting (83) into the last equation yields the result

$$J_{\xi_{n+1}} - J_{\xi_n} = 0 \tag{85}$$

Accordingly, generalized momentum maps of the form (51) are conserved in the discrete setting.

## 6. Numerical investigations

The main purpose of this section is to compare the numerical performance of the alternative numerical schemes developed in this work in the context of representative optimal control problems. The first numerical example deals with a three-dimensional mathematical pendulum formulated in terms of redundant coordinates. This prototypical example of a constrained mechanical system is well-suited to highlight important details distinguishing the alternative schemes under consideration. The second example deals with a closed-loop multibody system which can be modeled as mechanical system subject to holonomic constraints in a straightforward manner.

Our investigations cover the following five alternative schemes: The direct method applied in the framework of the common approach for $i = 2$ and $i = 3$ (Section 5.1), the indirect method applied in the framework of the maximum principle for $i = 3$

**Table 3**
Labeling of the 5 alternative schemes used in the numerical investigations.

| Label | Color | $i$ | $\alpha$ | Section | Method | in accord with |
|---|---|---|---|---|---|---|
| $\overline{\mathcal{H}}_3$ | • | 3 | 1 | 5.1 | direct | common approach |
| $\overline{\mathcal{H}}_2$ | • | 2 | 1 | 5.1 | direct | common approach |
| $\mathcal{H}_3$ | • | 3 | 1 | 5.2.1 | indirect | maximum principle |
| $\mathcal{H}_2$ | • | 2 | 1 | 5.2.2 | direct | maximum principle |
| $\mathcal{H}_2^{\mathrm{DD}}$ | • | 2 | $\frac{1}{2}$ | 5.2.3 | direct | maximum principle |

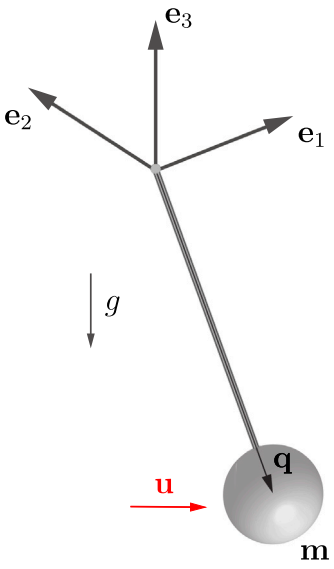


**Fig. 1.** The mathematical pendulum.

(Section 5.2.1), and the direct method [20] which overcomes the structural discrepancy as outlined in Section 5.2.2 for $i = 2$. We focus on first-order methods ($\alpha = 1$) to provide equal conditions for the comparison of these schemes. In addition to that, we apply the direct method based on the discrete derivative (Section 5.2.3, $i = 2$, $\alpha = \frac{1}{2}$), which also overcomes the structural discrepancy and yields second-order accuracy. The five alternative schemes under investigation are summarized in Table 3. The labeling of the schemes refers to the underlying Hamiltonian. That is, $\overline{\mathcal{H}}_i$ in (30), for the common approach, and $\mathcal{H}_i$ in (26), for the maximum principle. Specifically, we consider

$$\overline{\mathcal{H}}_3 = \overline{\lambda}_{3_{\mathbf{q}}}^T \mathbf{f}_3^{\mathbf{q}} + \overline{\lambda}_{3_{\mathbf{p}}}^T \mathbf{f}_3^{\mathbf{p}} + \overline{\boldsymbol{\eta}}_3^T \mathbf{g}_3 - C \tag{86a}$$

$$\overline{\mathcal{H}}_2 = \overline{\lambda}_{2_{\mathbf{q}}}^T \mathbf{f}_2^{\mathbf{q}} + \overline{\lambda}_{2_{\mathbf{p}}}^T \mathbf{f}_2^{\mathbf{p}} + \overline{\boldsymbol{\eta}}_2^T \mathbf{g}_2 - C \tag{86b}$$

$$\mathcal{H}_3 = \lambda_{3_{\mathbf{q}}}^T \mathbf{f}_3^{\mathbf{q}} + \lambda_{3_{\mathbf{p}}}^T \mathbf{f}_3^{\mathbf{p}} + \boldsymbol{\eta}_3^T \widetilde{\mathbf{g}}_3 - C \tag{86c}$$

$$\mathcal{H}_2 = \lambda_{2_{\mathbf{q}}}^T \mathbf{f}_2^{\mathbf{q}} + \lambda_{2_{\mathbf{p}}}^T \mathbf{f}_2^{\mathbf{p}} + \boldsymbol{\eta}_2^T \widetilde{\mathbf{g}}_2 - C \tag{86d}$$

For the purposes of this section we have enriched the notation of the adjoint variables to distinguish between the results of the alternative formulations under investigation.

Note that all of the schemes under consideration satisfy the constraints either on position level (for $i = 3$) or on both position and velocity level (for $i = 2$) at discrete time points $t_n$ ($n = 1, \dots, N$). In the numerical examples we focus on density cost functions of the form

$$C(\mathbf{u}) = \frac{1}{2}\mathbf{u}^T\mathbf{u} \tag{87}$$

All of the discrete conditions of optimality ($n = 1, \dots, N$) are solved as a monolithic algebraic system by applying Newton's method. Alternatively, a staggered solution scheme could be applied. We refer to [18] for a comparison of these two alternative solution procedures.

### 6.1. The mathematical pendulum

The first example deals with the three dimensional mathematical pendulum of length $l_0$ depicted in Fig. 1. Here, $\mathbf{q} \in \mathbb{R}^3$ is the position vector of the mass point $m$ and $\mathbf{p} \in \mathbb{R}^3$ is the conjugate momentum vector. There is one holonomic constraint which enforces the constant length of the pendulum:

$$g^q(\mathbf{q}) = \frac{1}{2}\left(\mathbf{q}^T\mathbf{q} - l_0^2\right) \tag{88}$$

The corresponding constraint on velocity level (2) is given by

$$g^v(\mathbf{q},\mathbf{p}) = \frac{1}{m}\mathbf{q}^T\mathbf{p} \tag{89}$$

where $m$ is the mass of the pendulum.

The motion of the pendulum takes place in the gravitational field, where $g$ is the gravitational acceleration. Correspondingly, the potential energy is given by

$$V(\mathbf{q}) = mg\mathbf{q}^T\mathbf{e}_3 \tag{90}$$

We next address the state DAEs summarized in Tables 1 and 2, respectively. Accordingly, the index-3 state DAEs ($i = 3$) hinge on the function

$$\mathbf{f}_3 = \begin{bmatrix}\mathbf{f}_3^{\mathbf{q}}\\ \mathbf{f}_3^{\mathbf{p}}\end{bmatrix} = \begin{bmatrix}\frac{1}{m}\mathbf{p}\\ -mg\mathbf{e}_3 - y_q\mathbf{q} + \mathbf{u}\end{bmatrix} \tag{91}$$

while the stabilized index-2 DAEs ($i = 2$) are based on

$$\mathbf{f}_2 = \begin{bmatrix}\mathbf{f}_2^{\mathbf{q}}\\ \mathbf{f}_2^{\mathbf{p}}\end{bmatrix} = \begin{bmatrix}\frac{1}{m}\mathbf{p} + \frac{y_v}{m}\mathbf{q}\\ -mg\mathbf{e}_3 - y_q\mathbf{q} - \frac{y_v}{m}\mathbf{p} + \mathbf{u}\end{bmatrix} \tag{92}$$

#### 6.1.1. Continuous conditions of optimality resulting from the common approach

For $i = 3$, the common approach is based on the Hamiltonian

$$\overline{\mathcal{H}}_3 = \overline{\lambda}_{3_{\mathbf{q}}}^T\mathbf{f}_3^{\mathbf{q}} + \overline{\lambda}_{3_{\mathbf{p}}}^T\mathbf{f}_3^{\mathbf{p}} + \overline{\eta}_3 g^q - C \tag{93}$$

where $\mathbf{f}_3^{\mathbf{q}}$ and $\mathbf{f}_3^{\mathbf{p}}$ are given by (91). Now, the adjoint DAEs read (cf. Section 3.3.2)

$$\dot{\overline{\lambda}}_{3_{\mathbf{q}}} = y_q\overline{\lambda}_{3_{\mathbf{p}}} - \overline{\eta}_3\mathbf{q} \tag{94a}$$

$$\dot{\overline{\lambda}}_{3_{\mathbf{p}}} = -\frac{1}{m}\overline{\lambda}_{3_{\mathbf{q}}} \tag{94b}$$

$$0 = \mathbf{q}^T\overline{\lambda}_{3_{\mathbf{p}}} \tag{94c}$$

together with the optimality condition

$$\mathbf{u} = \overline{\lambda}_{3_{\mathbf{p}}} \tag{95}$$

Note that (95) together with (94c) imply that $\mathbf{q}^T\mathbf{u} = 0$, so that the optimal control force is confined to the tangent plane $\mathcal{T}_q\mathcal{Q}$, where configuration space $\mathcal{Q}$ has been introduced in (1). Furthermore, formula (45) for the adjoint variable $\overline{\eta}_3$ yields

$$\overline{\eta}_3 = \frac{1}{l_0^2}\left(\frac{2}{m}\overline{\lambda}_{3_{\mathbf{q}}}^T\mathbf{p} + mg\overline{\lambda}_{3_{\mathbf{p}}}^T\mathbf{e}_3 - \overline{\lambda}_{3_{\mathbf{p}}}^T\mathbf{u}\right) \tag{96}$$

For $i = 2$, the underlying Hamiltonian reads

$$\overline{\mathcal{H}}_2 = \overline{\lambda}_{2_{\mathbf{q}}}^T\mathbf{f}_2^{\mathbf{q}} + \overline{\lambda}_{2_{\mathbf{p}}}^T\mathbf{f}_2^{\mathbf{p}} + \overline{\eta}_2^q g^q + \overline{\eta}_2^v g^v - C \tag{97}$$

where $\mathbf{f}_2^{\mathbf{q}}$ and $\mathbf{f}_2^{\mathbf{p}}$ are given by (92), and the constraint functions $g^q$ and $g^v$ assume the form in (88) and (89), respectively. The adjoint DAEs now follow as (cf. Section 3.3.2)

$$\dot{\overline{\lambda}}_{2_{\mathbf{q}}} = y_q\overline{\lambda}_{2_{\mathbf{p}}} - \overline{\eta}_2^q\mathbf{q} - \frac{\overline{\eta}_2^v}{m}\mathbf{p} \tag{98a}$$

$$\dot{\overline{\lambda}}_{2_{\mathbf{p}}} = -\frac{1}{m}\overline{\lambda}_{2_{\mathbf{q}}} - \frac{\overline{\eta}_2^v}{m}\mathbf{q} \tag{98b}$$

$$\mathbf{0} = \mathbf{q}^T\overline{\lambda}_{2_{\mathbf{p}}} \tag{98c}$$

$$\mathbf{0} = \mathbf{q}^T\overline{\lambda}_{2_{\mathbf{q}}} - \mathbf{p}^T\overline{\lambda}_{2_{\mathbf{p}}} \tag{98d}$$

along with the optimality condition

$$\mathbf{u} = \overline{\lambda}_{2_{\mathbf{p}}} \tag{99}$$

It can again be observed that the optimal control force is restricted to the tangent plane $\mathcal{T}_q\mathcal{Q}$. Following the procedure that led to (48), one obtains explicit formulas for the algebraic adjoint variables

$$\overline{\eta}_2^q = \frac{1}{l_0^2}\left(\frac{2}{m}\overline{\lambda}_{2_\mathbf{q}}^T\mathbf{p} + mg\overline{\lambda}_{2_\mathbf{p}}^T\mathbf{e}_3 - \overline{\lambda}_{2_\mathbf{p}}^T\mathbf{u}\right) \tag{100a}$$

$$\overline{\eta}_2^v = 0 \tag{100b}$$

### 6.1.2. Continuous conditions of optimality resulting from the maximum principle

For $i = 3$, the maximum principle is based on the Hamiltonian

$$\mathcal{H}_3 = \lambda_{3_\mathbf{q}}^T\mathbf{f}_3^\mathbf{q} + \lambda_{3_\mathbf{p}}^T\mathbf{f}_3^\mathbf{p} + \eta_3\tilde{g}_3 - C \tag{101}$$

where $\mathbf{f}_3^\mathbf{q}$ and $\mathbf{f}_3^\mathbf{p}$ are given by (91), and $\tilde{g}_3$ follows from definition (27) and thus assumes the form

$$\tilde{g}_3 = \frac{1}{m^2}\mathbf{p}^T\mathbf{p} + \frac{1}{m}\mathbf{q}^T\left(-mg\mathbf{e}_3 - y_q\mathbf{q} + \mathbf{u}\right)$$

The adjoint DAEs can now be calculated in a straightforward way and yield (cf. Section 3.3.1)

$$\dot{\lambda}_{3_\mathbf{q}} = y_q\lambda_{3_\mathbf{p}} + \frac{\eta_3}{m}\left(mg\mathbf{e}_3 + 2y_q\mathbf{q} - \mathbf{u}\right) \tag{102a}$$

$$\dot{\lambda}_{3_\mathbf{p}} = -\frac{1}{m}\lambda_{3_\mathbf{q}} - \frac{2\eta_3}{m^2}\mathbf{p} \tag{102b}$$

$$0 = \mathbf{q}^T\lambda_{3_\mathbf{p}} + \frac{l_0^2}{m}\eta_3 \tag{102c}$$

together with the optimality condition

$$\mathbf{u} = \lambda_{3_\mathbf{p}} + \frac{\eta_3}{m}\mathbf{q} \tag{103}$$

From (102c) follows

$$\eta_3 = -\frac{m}{l_0^2}\mathbf{q}^T\lambda_{3_\mathbf{p}} \tag{104}$$

which is the pendulum-specific version of (38). Inserting the last equation into (103) leads to the relationship

$$\mathbf{u} = \left(\mathbf{I} - \frac{1}{l_0^2}\mathbf{q}\mathbf{q}^T\right)\lambda_{3_\mathbf{p}} \tag{105}$$

Accordingly, the optimal control vector $\mathbf{u}$ equals the orthogonal projection of the adjoint variable $\lambda_{3_\mathbf{p}}$ onto the tangent plane $\mathcal{T}_q\mathcal{Q}$, which again implies $\mathbf{q}^T\mathbf{u} = 0$.

For $i = 2$, the underlying Hamiltonian is given by

$$\mathcal{H}_2 = \lambda_{2_\mathbf{q}}^T\mathbf{f}_2^\mathbf{q} + \lambda_{2_\mathbf{p}}^T\mathbf{f}_2^\mathbf{p} + \eta_2^v\tilde{g}_2^v + \eta_2^a\tilde{g}_2^a - C \tag{106}$$

where $\mathbf{f}_2^\mathbf{q}$ and $\mathbf{f}_2^\mathbf{p}$ are given by (92). Moreover, $\tilde{g}_2^v$ and $\tilde{g}_2^a$ are the component expressions of (28), leading to

$$\tilde{g}_2^v = \mathbf{q}^T\left(\frac{1}{m}\mathbf{p} + \frac{y_v}{m}\mathbf{q}\right) \tag{107a}$$

$$\tilde{g}_2^a = \frac{1}{m^2}\mathbf{p}^T\mathbf{p} + \frac{1}{m}\mathbf{q}^T\left(-mg\mathbf{e}_3 - y_q\mathbf{q} + \mathbf{u}\right) \tag{107b}$$

The adjoint DAEs can now be obtained as (cf. Section 3.3.1)

$$\dot{\lambda}_{2_\mathbf{q}} = y_q\lambda_{2_\mathbf{p}} - \frac{\eta_2^v}{m}\mathbf{p} + \frac{\eta_2^a}{m}\left(mg\mathbf{e}_3 + 2y_q\mathbf{q} - \mathbf{u}\right) \tag{108a}$$

$$\dot{\lambda}_{2_\mathbf{p}} = -\frac{1}{m}\lambda_{2_\mathbf{q}} - \frac{\eta_2^v}{m}\mathbf{q} - \frac{2\eta_2^a}{m^2}\mathbf{p} \tag{108b}$$

$$0 = \mathbf{q}^T\lambda_{2_\mathbf{p}} + \frac{l_0^2}{m}\eta_2^a \tag{108c}$$

$$0 = \mathbf{q}^T\lambda_{2_\mathbf{q}} - \mathbf{p}^T\lambda_{2_\mathbf{p}} + l_0^2\eta_2^v \tag{108d}$$

together with the optimality condition

$$\mathbf{u} = \lambda_{2_\mathbf{p}} + \frac{\eta_2^a}{m}\mathbf{q} \tag{109}$$

From (108c) and (108d) one obtains

$$\eta_2^v = \frac{1}{l_0^2}\left(\mathbf{p}^T\lambda_{2_\mathbf{p}} - \mathbf{q}^T\lambda_{2_\mathbf{q}}\right) \tag{110a}$$

**Table 4**
Pendulum: data used in the numerical example.

| | | |
|---|---|---|
| $m$ | 1 | Mass of the particle |
| $g$ | 9.81 | Gravitational acceleration |
| $l_0$ | 5 | Length of the pendulum |
| $\bar{\mathbf{q}}_0$ | $(5,0,0)$ | Initial position |
| $\bar{\mathbf{p}}_0$ | $(0,10,0)$ | Initial momentum |
| $\bar{\mathbf{q}}_N$ | $(0,0,-5)$ | Final position |
| $\bar{\mathbf{p}}_N$ | $(0,0,0)$ | Final momentum |
| $T$ | 1 | Final time |
| $N$ | 100 | Number of time steps |

$$\eta_2^a = -\frac{m}{l_0^2}\mathbf{q}^T\lambda_{2_\mathbf{p}} \tag{110b}$$

which corresponds to the pendulum-specific version of (40). Inserting the last equation into (109) yields

$$\mathbf{u} = \left(\mathbf{I} - \frac{1}{l_0^2}\mathbf{q}\mathbf{q}^T\right)\lambda_{2_\mathbf{p}} \tag{111}$$

Accordingly, the optimal control vector $\mathbf{u}$ equals the orthogonal projection of the adjoint variable $\lambda_{2_\mathbf{p}}$ onto the tangent plane $\mathcal{T}_q\mathcal{Q}$, which again implies $\mathbf{q}^T\mathbf{u} = 0$.

### 6.1.3. Symmetry and generalized momentum maps

It can be observed from (90) that the potential energy is invariant with respect to rotations of the pendulum about the $\mathbf{e}_3$-axis. That is, $V(\mathbf{q}) = V(\mathbf{R}^s\mathbf{q})$, where $\mathbf{R}^s \in SO(3)$ represents rotations about the $\mathbf{e}_3$-axis. Correspondingly, $G = SO(3)$ is the special orthogonal group in $\mathbb{R}^3$, and rotation matrix $\mathbf{R}^s \in SO(3)$ can be expressed as $\mathbf{R}^s = \exp(s\hat{\mathbf{e}}_3)$, where $\hat{\mathbf{e}}_3 \in \mathfrak{g} \equiv so(3)$ is a skew-symmetric matrix with associated axial vector $\mathbf{e}_3$ satisfying $\hat{\mathbf{e}}_3\mathbf{a} = \mathbf{e}_3 \times \mathbf{a}$ for any vector $\mathbf{a} \in \mathbb{R}^3$. The group action considered in Proposition 1 corresponds to the cotangent lifted action of $SO(3)$ on phase space $\mathcal{P}$ given by

$$\Phi_{\mathbf{R}^s}(\mathbf{x}) = \begin{bmatrix}\mathbf{R}^s\mathbf{q}\\ \mathbf{R}^{s^{-T}}\mathbf{p}\end{bmatrix} = \begin{bmatrix}\mathbf{R}^s\mathbf{q}\\ \mathbf{R}^s\mathbf{p}\end{bmatrix}$$

The last equation implies

$$D\Phi_{\mathbf{R}^s}(\mathbf{x}) = \begin{bmatrix}\mathbf{R}^s & \mathbf{0}\\ \mathbf{0} & \mathbf{R}^s\end{bmatrix}$$

It can now be easily verified that all of the symmetry conditions (50) in Proposition 1 are satisfied by choosing $\mathbf{u}^s = \mathbf{R}^s\mathbf{u}$ and $\mathbf{y}_i^s = \mathbf{y}_i$. Accordingly, the symmetry of the underlying uncontrolled mechanical system is inherited by the optimal control problem. Calculating the infinitesimal generator (49) yields

$$\xi_\mathcal{P}(\mathbf{x}) = \left.\frac{\mathrm{d}}{\mathrm{d}s}\right|_{s=0}\Phi_{g^s}(\mathbf{x}) = \begin{bmatrix}\mathbf{e}_3\times\mathbf{q}\\ \mathbf{e}_3\times\mathbf{p}\end{bmatrix}$$

so that the generalized momentum map (51) assumes the form

$$J_{\mathbf{e}_3}(\mathbf{x},\lambda) = \mathbf{e}_3\cdot\left(\mathbf{q}\times\lambda_\mathbf{q} + \mathbf{p}\times\lambda_\mathbf{p}\right)$$

We call the quadratic function

$$\mathbf{J}(\mathbf{x},\lambda) = \mathbf{q}\times\lambda_\mathbf{q} + \mathbf{p}\times\lambda_\mathbf{p} \tag{112}$$

the generalized angular momentum. According to Proposition 1, the 3-component of $\mathbf{J}$ is a conserved quantity of the optimal control problem.

### 6.1.4. Numerical results

The goal of the optimal control problem under investigation is to determine the maneuver from the prescribed initial state $(\bar{\mathbf{q}}_0, \bar{\mathbf{p}}_0)$ to the prescribed final state $(\bar{\mathbf{q}}_N, \bar{\mathbf{p}}_N)$ within the prescribed time interval $I \in [0,T]$. As defined in (87), the maneuver is to be carried out with a minimal control effort. The data used in the numerical example is summarized in Table 4. Consistent initial values for the Lagrange multiplier $y_q$ can be obtained from (8), leading to the formula

$$y_q = \frac{1}{l_0^2}\left(\frac{1}{m}\mathbf{p}^T\mathbf{p} - mg\mathbf{q}^T\mathbf{e}_3\right)$$

All of the numerical schemes under investigation essentially yield the same results for the mechanical quantities. This can be seen from Figs. 2 and 3, where the results for the coordinates, the momenta, the controls and the Lagrange multiplier $y_q$ are shown.

The fulfillment of the mechanical constraints on position level, velocity level and acceleration level is depicted in Fig. 4. As expected, all schemes satisfy the constraints on position level up to numerical round-off, while the constraints on velocity level are

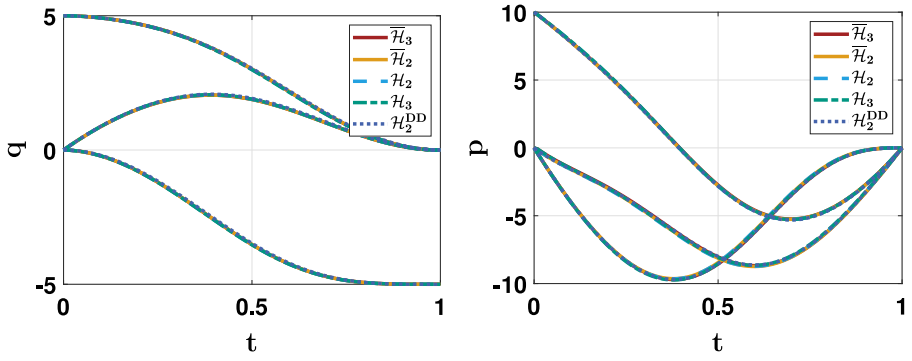


**Fig. 2.** Evolution of the coordinates $\mathbf{q}$ and the momenta $\mathbf{p}$ over time. The assignment of the various solutions for $\mathbf{q} = \left(q^1, q^2, q^3\right)^T$ and $\mathbf{p} = \left(p^1, p^2, p^3\right)^T$ can be obtained from the boundary conditions in Table 4.

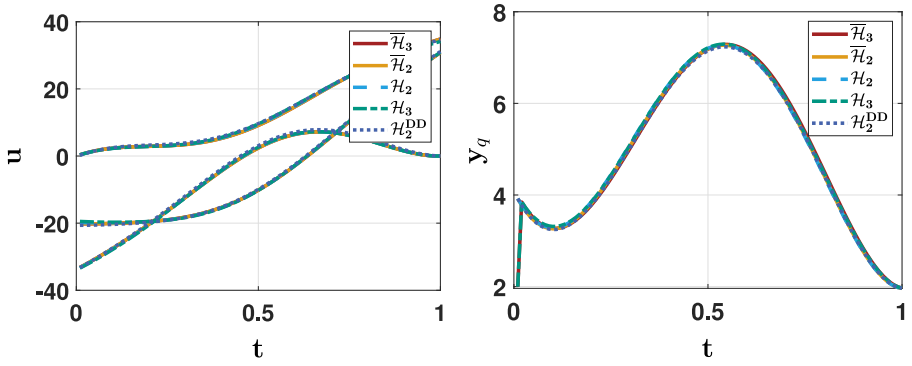


**Fig. 3.** Evolution of the controls $\mathbf{u}$ with initial values $\mathbf{u}(t_0) = (0, -20, -33)^T$ and Lagrange multiplier $\mathbf{y}_q$ over time.

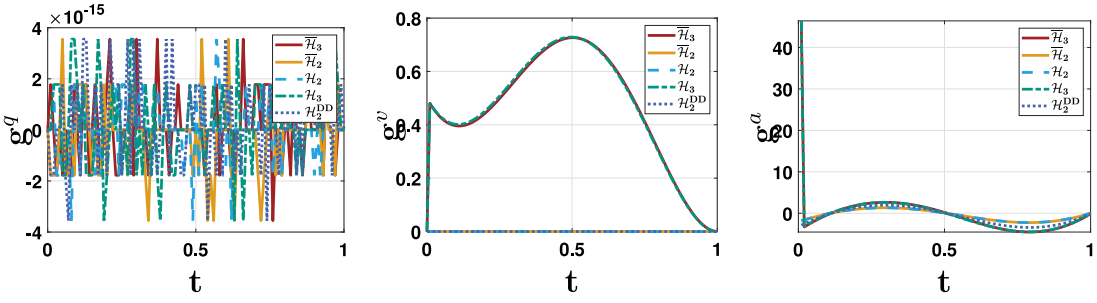


**Fig. 4.** Fulfillment of the constraints on position level $\mathbf{g}^q$, on velocity level $\mathbf{g}^v$ and on acceleration level $\mathbf{g}^a$.

only met by the schemes based on the stabilized index-2 state DAEs (the schemes labeled with $\overline{\mathcal{H}}_2$, $\mathcal{H}_2$, and $\mathcal{H}_2^{\mathrm{DD}}$). The motion of the pendulum is visualized in Fig. 5 by means of some snapshots in time.

The time-evolution of the differential adjoint variables $\lambda_2$ and $\overline{\lambda}_2$ is shown in Fig. 6, while the evolution of $\lambda_3$ and $\overline{\lambda}_3$ is depicted in Fig. 7. The time-evolution of the algebraic adjoint variables $\boldsymbol{\eta}_2$, $\overline{\boldsymbol{\eta}}_2$, $\eta_3$, and $\overline{\eta}_3$ is shown in Fig. 8.

The numerical results for the time-evolution of the optimal control Hamiltonians are depicted in Fig. 9. Although none of the schemes under investigation is capable to exactly conserve the Hamiltonian of the optimal control problem, the newly proposed scheme labeled with $\mathcal{H}_2^{\mathrm{DD}}$ already achieves almost conserving results. If the time steps are refined, all of the schemes at hand converge to the same constant value of the optimal control Hamiltonian.

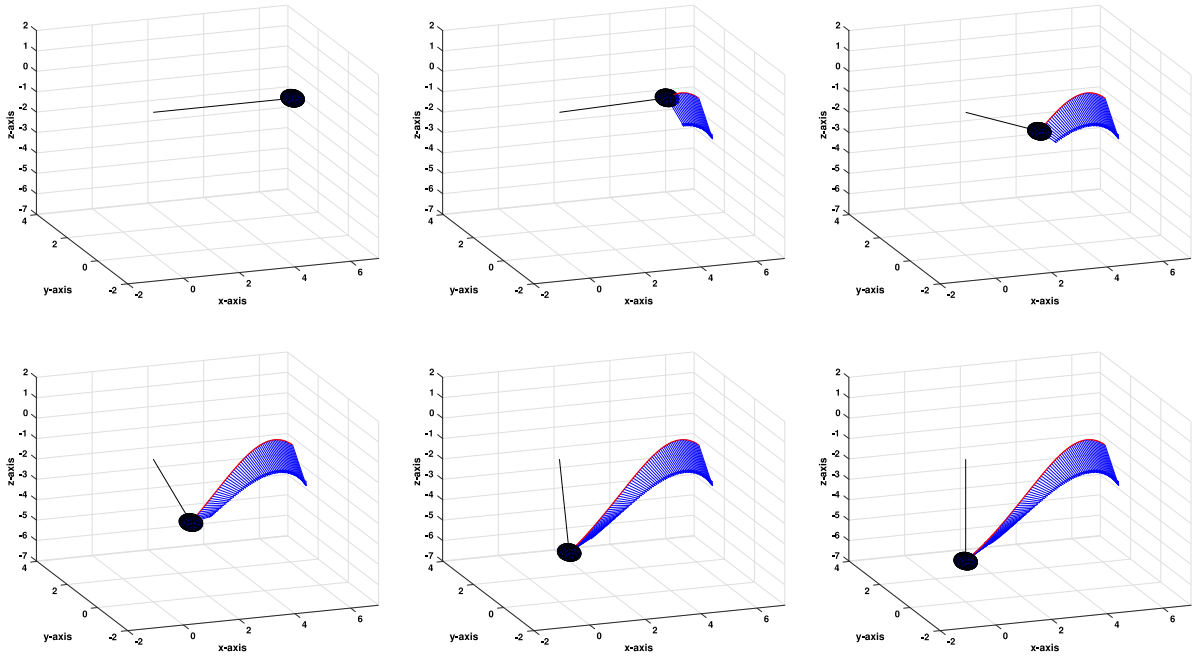


**Fig. 5.** Snapshots of the optimal motion at $t \in \{0,\ 0.2,\ 0.4,\ 0.6,\ 0.8,\ 1\}$. The trajectory of the mass point is shown with red lines, while the control vector $\mathbf{u}$ is indicated with blue arrows.

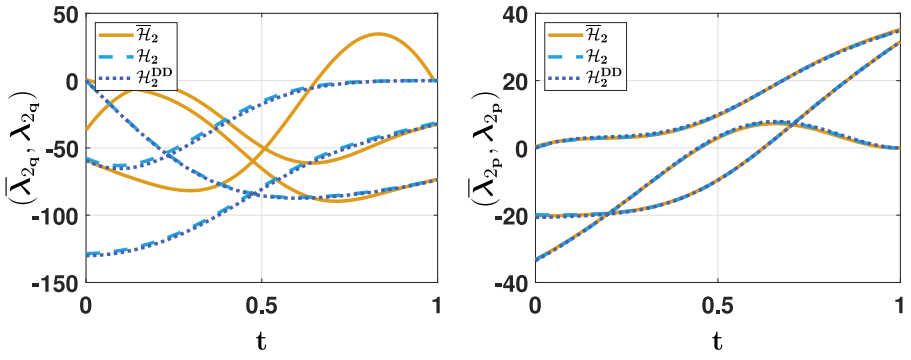


**Fig. 6.** Evolution of the adjoint variables $\lambda_2 = (\lambda_{2_q}, \lambda_{2_p})$ and $\overline{\lambda}_2 = (\overline{\lambda}_{2_q}, \overline{\lambda}_{2_p})$. To identify the corresponding solutions of $\lambda_2$, the points $\left(\overline{\lambda}_{2_q}(t_f), \lambda_{2_q}(t_f)\right)$ are about $(-31, -73, 0)$ and the points $\left(\overline{\lambda}_{2_p}(t_f), \lambda_{2_p}(t_f)\right)$ are about $(35, 31, 0)$.

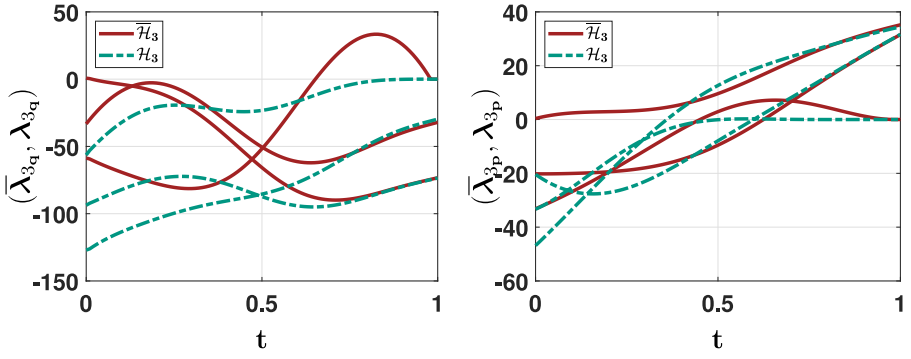


**Fig. 7.** Evolution of the adjoint variables $\lambda_3 = (\lambda_{3_q}, \lambda_{3_p})$ and $\overline{\lambda}_3 = (\overline{\lambda}_{3_q}, \overline{\lambda}_{3_p})$.

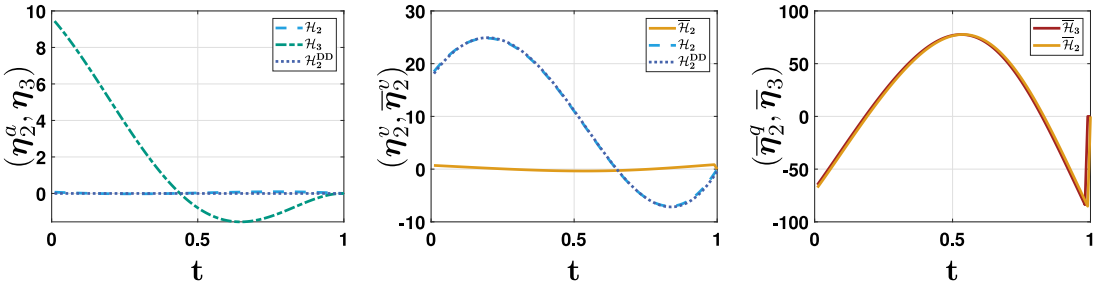


**Fig. 8.** Evolution of the adjoint variables $\boldsymbol{\eta}_2 = (\eta_2^v, \eta_2^a)$, $\overline{\boldsymbol{\eta}}_2 = (\overline{\eta}_2^q, \overline{\eta}_2^v)$, $\eta_3$, and $\overline{\eta}_3$.

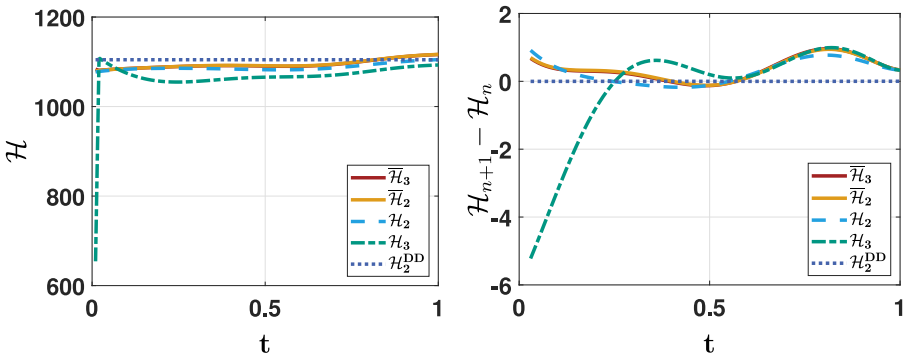


**Fig. 9.** Evolution of the optimal control Hamiltonian (left), and incremental change of the optimal control Hamiltonian (right).

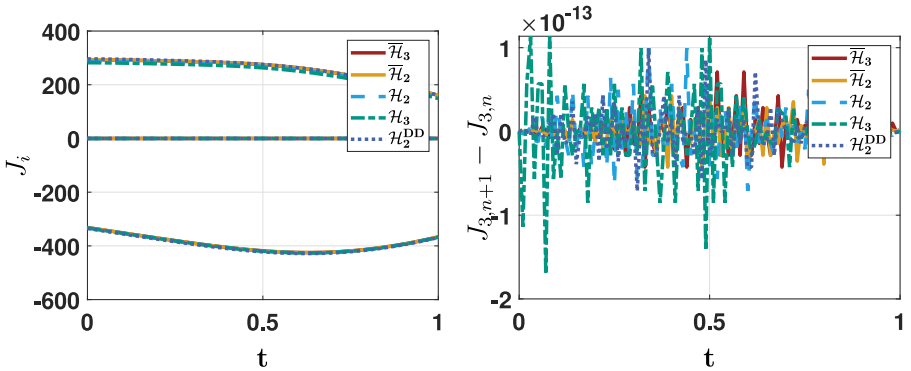


**Fig. 10.** Evolution of the components of the generalized angular momentum $\mathbf{J} = \mathbf{q} \times \lambda_{\mathbf{q}} + \mathbf{p} \times \lambda_{\mathbf{p}}$ over time (left). To $\mathbf{J} = (J_1, J_2, J_3)$ corresponding solutions can by identified by the initial point $\mathbf{J}(t_0)$, which is about $\mathbf{J}(t_0) = (-333, 290, 0)$. The 3-component $J_3 = \mathbf{e}_3^T \mathbf{J}$ is a conserved quantity of the present optimal control problem. This is corroborated by the incremental changes of $J_3$ (right).

The results for the generalized angular momentum $\mathbf{J} = \mathbf{q} \times \lambda_{\mathbf{q}} + \mathbf{p} \times \lambda_{\mathbf{p}}$ are depicted in Fig. 10. As shown in Section 6.1.3, the 3-component of $\mathbf{J}$ is a conserved quantity. As expected (cf. Section 5.3), all of the schemes under investigation are capable to conserve $J_3 = \mathbf{e}_3^T \mathbf{J}$.

Eventually, the convergence behavior of the different schemes at hand is compared in Fig. 11. To this end, the relative error in the state variables and the controls is calculated via

$$\varepsilon_{\mathbf{x}} = \frac{\|\mathbf{x}(t=0.5) - \mathbf{x}_{\mathrm{ref}}(t=0.5)\|_{L_2}}{\|\mathbf{x}_{\mathrm{ref}}(t=0.5)\|_{L_2}}; \qquad \varepsilon_{\mathbf{u}} = \frac{\|\mathbf{u}(t=0.5) - \mathbf{u}_{\mathrm{ref}}(t=0.5)\|_{L_2}}{\|\mathbf{u}_{\mathrm{ref}}(t=0.5)\|_{L_2}} \tag{113}$$

where the reference solution was calculated with scheme $\mathcal{H}_2^{\mathrm{DD}}$ and $N = 100.000$ time intervals. As expected, the schemes based on $\alpha = 1$ yield first-order accuracy in the state variables, while $\mathcal{H}_2^{\mathrm{DD}}$ yields second-order accuracy. Analogous convergence results are obtained for the differential adjoint variables. The observed equal order of convergence of the state and adjoint variables complies with theoretical results for the application of symplectic integrators to the optimal control of ODEs, see [7] and the references

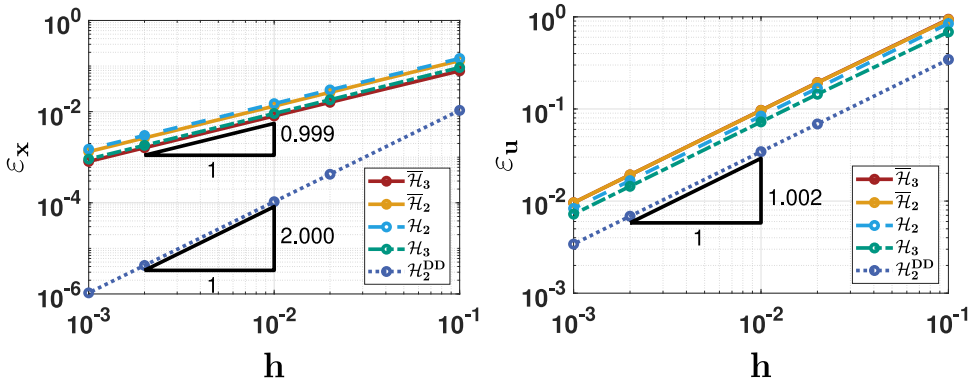


**Fig. 11.** Convergence behavior of the alternative schemes.

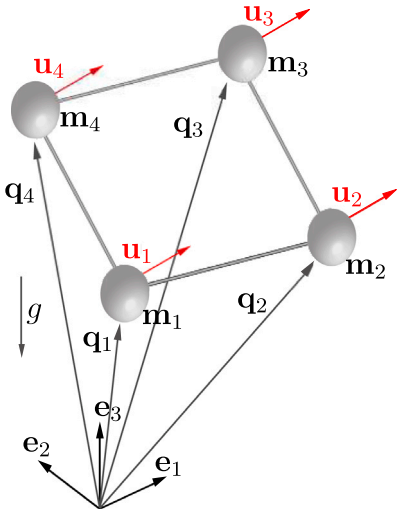


**Fig. 12.** Sketch of the four linked masses.

therein. All schemes are first-order accurate in the controls. Similar results hold for other variables whose discretization relies on constant values per time step, such as the mechanical Lagrange multipliers and the algebraic adjoint variables.

### 6.2. Four linked masses

This example deals with 4 mass points $m_k$ $(k = 1, \dots, 4)$, which are linked to each other by massless rigid bars as depicted in Fig. 12. A preliminary version of this example has been dealt with in [32]. Redundant coordinates offer a versatile and general approach to model this type of closed kinematic chain. In particular, the configuration vector of the closed-loop system at hand is given by

$$\mathbf{q} = \begin{bmatrix} \mathbf{q}_1 \\ \mathbf{q}_2 \\ \mathbf{q}_3 \\ \mathbf{q}_4 \end{bmatrix} \tag{114}$$

where $\mathbf{q}_k \in \mathbb{R}^3$ is the position vector of particle $m_k$ with respect to a Cartesian inertial frame.

The mass point system is subject to four holonomic constraints of the form

$$g_k^q(\mathbf{q}) = \frac{1}{2}\left(\Delta\mathbf{q}_k^T \Delta\mathbf{q}_k - l_0^2\right) = 0 \tag{115}$$

$(k = 1, \dots, 4)$, where $\Delta\mathbf{q}_1 = \mathbf{q}_2 - \mathbf{q}_1$, $\Delta\mathbf{q}_2 = \mathbf{q}_3 - \mathbf{q}_2$, $\Delta\mathbf{q}_3 = \mathbf{q}_4 - \mathbf{q}_3$, and $\Delta\mathbf{q}_4 = \mathbf{q}_1 - \mathbf{q}_4$. Note that $g_4^q(\mathbf{q}) = 0$ can be viewed as loop-closure condition. The conjugate linear momentum is given by $\mathbf{p} = \mathbf{M}\dot{\mathbf{q}}$, where the $12 \times 12$ mass matrix $\mathbf{M}$ is diagonal such that $\mathbf{p}_k = m_k \dot{\mathbf{q}}_k$.

The four constraints on velocity level assume the form (2), where the components are given by $g_k^v = Dg_k^q(\mathbf{q})\mathbf{M}^{-1}\mathbf{p} = \mathbf{0}$ $(k = 1, \dots, 4)$. Gravity is acting on the system leading to the potential energy

$$V(\mathbf{q}) = \sum_{k=1}^{4} V_k(\mathbf{q}_k) \quad \text{where} \quad V_k(\mathbf{q}_k) = m_k g \mathbf{q}_k^T \mathbf{e}_3 \tag{116}$$

In addition to that, four control forces $\mathbf{u}_k \in \mathbb{R}^3$ $(k = 1, \dots, 4)$ are acting on the corresponding mass points $m_k$.

### 6.2.1. Symmetry and generalized momentum maps

*Rotational symmetry.* Similarly to the last example, the uncontrolled mass point system has rotational symmetry about the $\mathbf{e}_3$ axis. The rotational symmetry is characterized by $V_k(\mathbf{R}^s\mathbf{q}_k) = V_k(\mathbf{q}_k)$, where rotation matrix $\mathbf{R}^s \in SO(3)$ can again be written in the form $\mathbf{R}^s = \exp(s\widehat{\mathbf{e}}_3)$. The group action considered in Proposition 1 can be characterized by

$$\Phi_{\mathbf{R}^s}(\mathbf{x}_k) = \begin{bmatrix} \mathbf{R}^s & \mathbf{0} \\ \mathbf{0} & \mathbf{R}^s \end{bmatrix} \mathbf{x}_k$$

where $\mathbf{x}_k = (\mathbf{q}_k, \mathbf{p}_k)$ $(k = 1, \dots, 4)$. It is now straightforward to verify that all of the symmetry conditions (50) in Proposition 1 are satisfied by choosing $\mathbf{u}_k^s = \mathbf{R}^s\mathbf{u}_k$ and $\mathbf{y}_{i_k}^s = \mathbf{y}_{i_k}$, where $\mathbf{y}_{i_k}$ denotes the Lagrange multiplier associated with constraint function $\mathbf{g}_{i_k}$ for $k = 1, \dots, 4$ and $i \in \{2, 3\}$. The infinitesimal generator (49) can be characterized by

$$\xi_{\mathcal{P}}(\mathbf{x}_k) = \left.\frac{\mathrm{d}}{\mathrm{d}s}\right|_{s=0} \Phi_{\mathbf{R}^s}(\mathbf{x}_k) = \begin{bmatrix} \widehat{\mathbf{e}}_3 & \mathbf{0} \\ \mathbf{0} & \widehat{\mathbf{e}}_3 \end{bmatrix} \mathbf{x}_k$$

so that the generalized momentum map (51) can be written in the form

$$\begin{aligned} J_3(\mathbf{x}, \lambda) &= \sum_{k=1}^{4} \lambda^{k^T} \xi_{\mathcal{P}}(\mathbf{x}_k) \\ &= \sum_{k=1}^{4} \left( \lambda_{\mathbf{q}}^{k^T} \widehat{\mathbf{e}}_3 \mathbf{q}_k + \lambda_{\mathbf{p}}^{k^T} \widehat{\mathbf{e}}_3 \mathbf{p}_k \right) \\ &= \mathbf{e}_3^T \sum_{k=1}^{4} \left( \mathbf{q}_k \times \lambda_{\mathbf{q}}^k + \mathbf{p}_k \times \lambda_{\mathbf{p}}^k \right) \end{aligned}$$

where the adjoint variables associated with mass point $m_k$ have been partitioned according to $\lambda^k = (\lambda_{\mathbf{q}}^k, \lambda_{\mathbf{p}}^k)$. Accordingly, the 3-component of the generalized angular momentum

$$\mathbf{J} = \sum_{k=1}^{4} \left( \mathbf{q}_k \times \lambda_{\mathbf{q}}^k + \mathbf{p}_k \times \lambda_{\mathbf{p}}^k \right) \tag{117}$$

is a conserved quantity of the optimal control problem.

*Translational symmetry.* The optimal control problem of the mass point system at hand has also translational symmetry that can be characterized by $\mathbf{q}_k^s = \mathbf{q}_k + s\boldsymbol{\xi}$, for any $\boldsymbol{\xi} \in \mathbb{R}^3$. The corresponding cotangent lifted action of the additive group $\mathbb{R}^3$ on phase space $\mathcal{P}$ can now be characterized by

$$\Phi_{\xi^s}(\mathbf{x}_k) = \begin{bmatrix} \mathbf{q}_k + s\boldsymbol{\xi} \\ \mathbf{p}_k \end{bmatrix}$$

so that infinitesimal generator (49) gives rise to

$$\xi_{\mathcal{P}}(\mathbf{x}_k) = \left.\frac{\mathrm{d}}{\mathrm{d}s}\right|_{s=0} \Phi_{\xi^s}(\mathbf{x}_k) = \begin{bmatrix} \boldsymbol{\xi} \\ \mathbf{0} \end{bmatrix}$$

It can be easily verified that all of the symmetry conditions (50) in Proposition 1 are satisfied by choosing $\mathbf{u}_k^s = \mathbf{u}_k$ and $\mathbf{y}_{i_k}^s = \mathbf{y}_{i_k}$. The generalized momentum map (51) yields

$$L_{\xi}(\mathbf{x}, \lambda) = \sum_{k=1}^{4} \lambda^{k^T} \xi_{\mathcal{P}}(\mathbf{x}_k) = \sum_{k=1}^{4} \lambda_{\mathbf{q}}^{k^T} \boldsymbol{\xi} = \boldsymbol{\xi}^T \sum_{k=1}^{4} \lambda_{\mathbf{q}}^k$$

Accordingly, all of the three components of the generalized linear momentum

$$\mathbf{L} = \sum_{k=1}^{4} \lambda_{\mathbf{q}}^k \tag{118}$$

are conserved along solutions of the optimal control problem.

### 6.2.2. Numerical results

The boundary conditions $(\mathbf{q}_0, \mathbf{p}_0)$ and $(\mathbf{q}_N, \mathbf{p}_N)$, the time interval $I \in [0,\ T]$, and the number of time steps $N$ that have been used in the numerical example can be found in Table 5. Accordingly, while the initial configuration of the 4-mass system lies in the x–y plane, a rotational and translational motion is required to reach the final configuration of the system, which lies in the y–z plane.

As in the last example, all of the numerical schemes under investigation essentially yield the same results concerning the mechanical quantities. For example, the results for the position vectors $\mathbf{q}_k$ and linear momentum vectors $\mathbf{p}_k$ are depicted in Figs. 13 and 14, respectively.

**Table 5**
Four linked masses: data used in the numerical example.

| | | |
|---|---|---|
| $m$ | $[1;1;1;1]$ | Masses |
| $g$ | 9.81 | Grav. acceleration |
| $l_0$ | 1 | Length of the bars |
| $[\bar{q}_0^1;\bar{q}_0^2;\bar{q}_0^3;\bar{q}_0^4]$ | $[(-\frac{1}{2},-\frac{1}{2},0)\ ;\ (\frac{1}{2},-\frac{1}{2},0)\ ;\ (\frac{1}{2},\frac{1}{2},0)\ ;\ (-\frac{1}{2},\frac{1}{2},0)]$ | Initial positions |
| $[\bar{p}_0^1;\bar{p}_0^2;\bar{p}_0^3:\bar{p}_0^4]$ | $[(0,0,0)\ ;\ (0,0,0)\ ;\ (0,0,0)\ ;\ (0,0,0)]$ | Initial momenta |
| $[\bar{q}_N^1;\bar{q}_N^2;\bar{q}_N^3;\bar{q}_N^4]$ | $[(\frac{1}{2},-\frac{1}{2},1)\ ;\ (\frac{1}{2},\frac{1}{2},1)\ ;\ (\frac{1}{2},\frac{1}{2},2)\ ;\ (\frac{1}{2},-\frac{1}{2},2)]$ | Final positions |
| $[\bar{p}_N^1;\bar{p}_N^2;\bar{p}_N^3;\bar{p}_N^4]$ | $[(0,0,0)\ ;\ (0,0,0)\ ;\ (0,0,0)\ ;\ (0,0,0)]$ | Final momenta |
| $T$ | 1 | Final time |
| $N$ | 100 | Number of time steps |

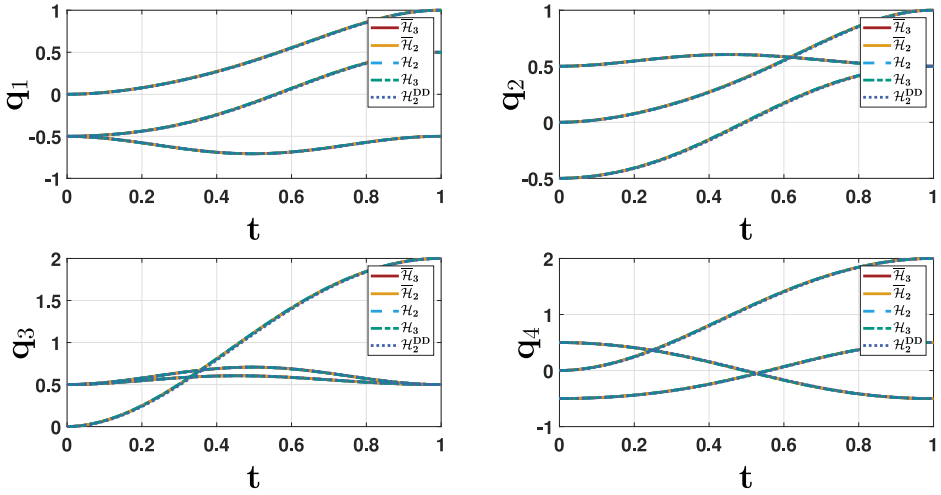


**Fig. 13.** Evolution of the coordinates of the four mass points over time.

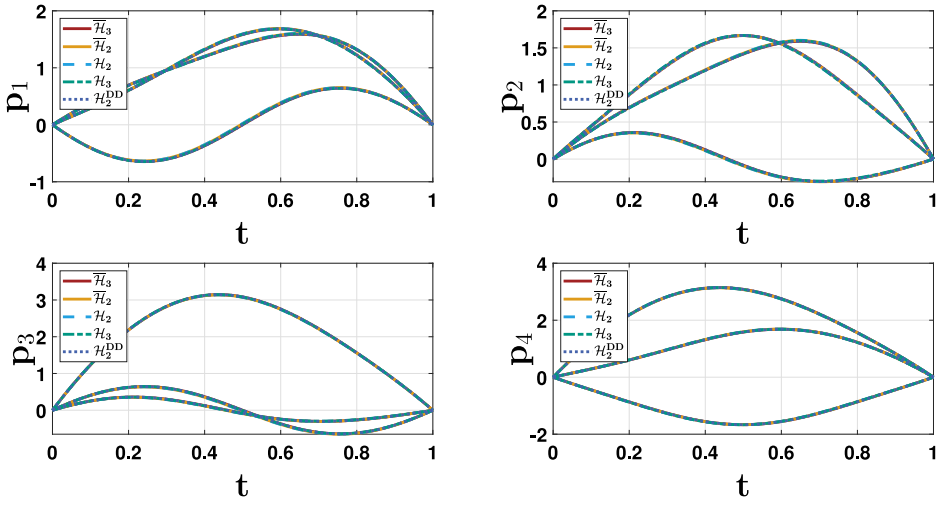


**Fig. 14.** Evolution of the linear momenta of the four mass points over time.

Moreover, the results for the four control vectors $\mathbf{u}_k$ are shown in Fig. 15.

Interestingly, the numerical results for the time-evolution of the Lagrange multipliers $y_q^k$ coincide for $k = 1,\dots,4$ (Fig. 16). This means that the constraint forces in the four bars are equal to each other over the course of the simulation. The motion is illustrated with a number of snapshots of the system over time in Fig. 18.

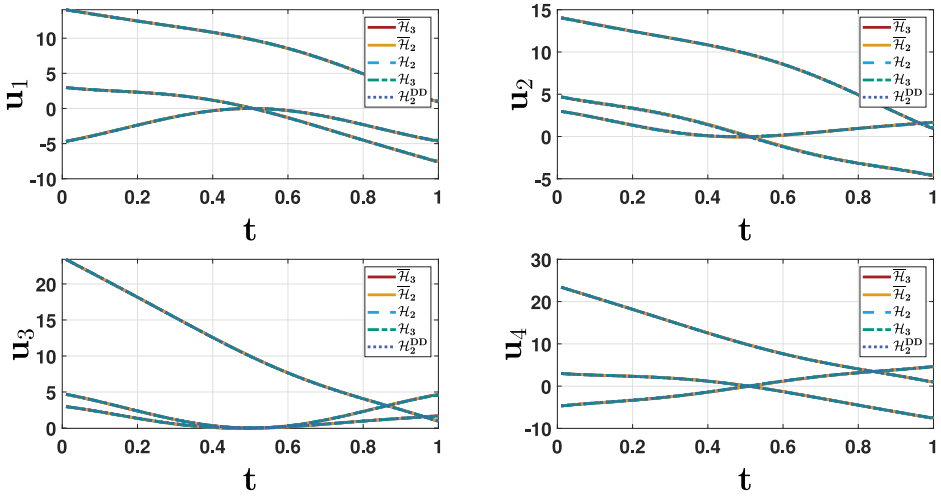


**Fig. 15.** Evolution of the controls over time. In order to identify the solutions of $\mathbf{u}_i(t)$, the initial values of the various results are about $\mathbf{u}_1(t_0) = (3, -5, 14)^T$, $\mathbf{u}_2(t_0) = (3, 5, 14)^T$, $\mathbf{u}_3(t_0) = (3, 5, 23)^T$ and $\mathbf{u}_4(t_0) = (3, -5, 23)^T$.

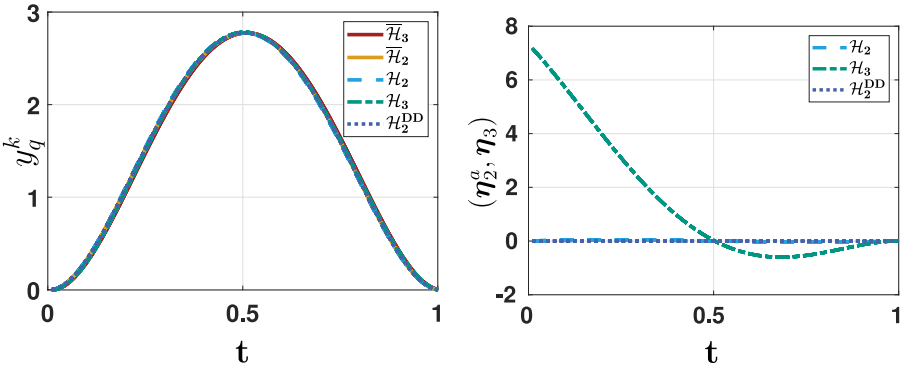


**Fig. 16.** Results for the Lagrange multipliers $y_q^k$ (left) and algebraic adjoint variables $(\boldsymbol{\eta}_2^a, \boldsymbol{\eta}_3)$ (right).

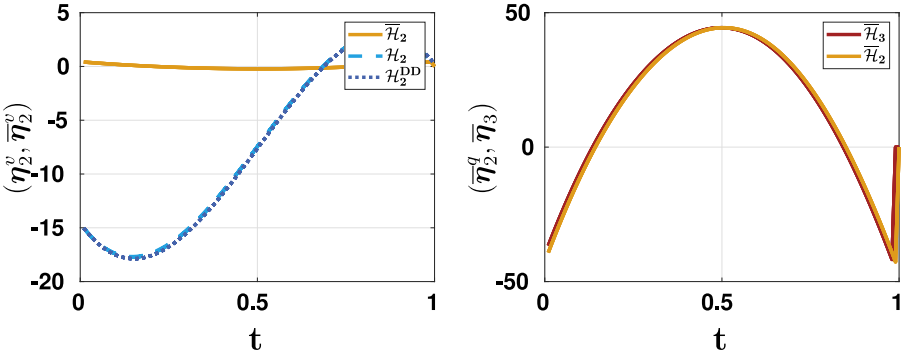


**Fig. 17.** Results for the algebraic adjoint variables $(\boldsymbol{\eta}_2^v, \overline{\boldsymbol{\eta}}_2^v)$ and $(\overline{\boldsymbol{\eta}}_2^q, \overline{\boldsymbol{\eta}}_3)$.

The time-evolution of the differential adjoint variables $\boldsymbol{\lambda}_{\mathbf{p}}^k$ and $\boldsymbol{\lambda}_{\mathbf{q}}^k$ is depicted in Figs. 19 and 20, respectively. The time-evolution of the algebraic adjoint variables $\boldsymbol{\eta}_2$, $\overline{\boldsymbol{\eta}}_2$, $\eta_3$, and $\overline{\eta}_3$ is shown in Figs. 16 and 17.

The numerical results for the optimal control Hamiltonians are shown in Fig. 21. As in the last example, the scheme labeled with $\mathcal{H}_2^{\mathrm{DD}}$ yields already much better results than the other ones. If the time steps are refined, all of the schemes at hand converge to the same constant value of the optimal control Hamiltonian.

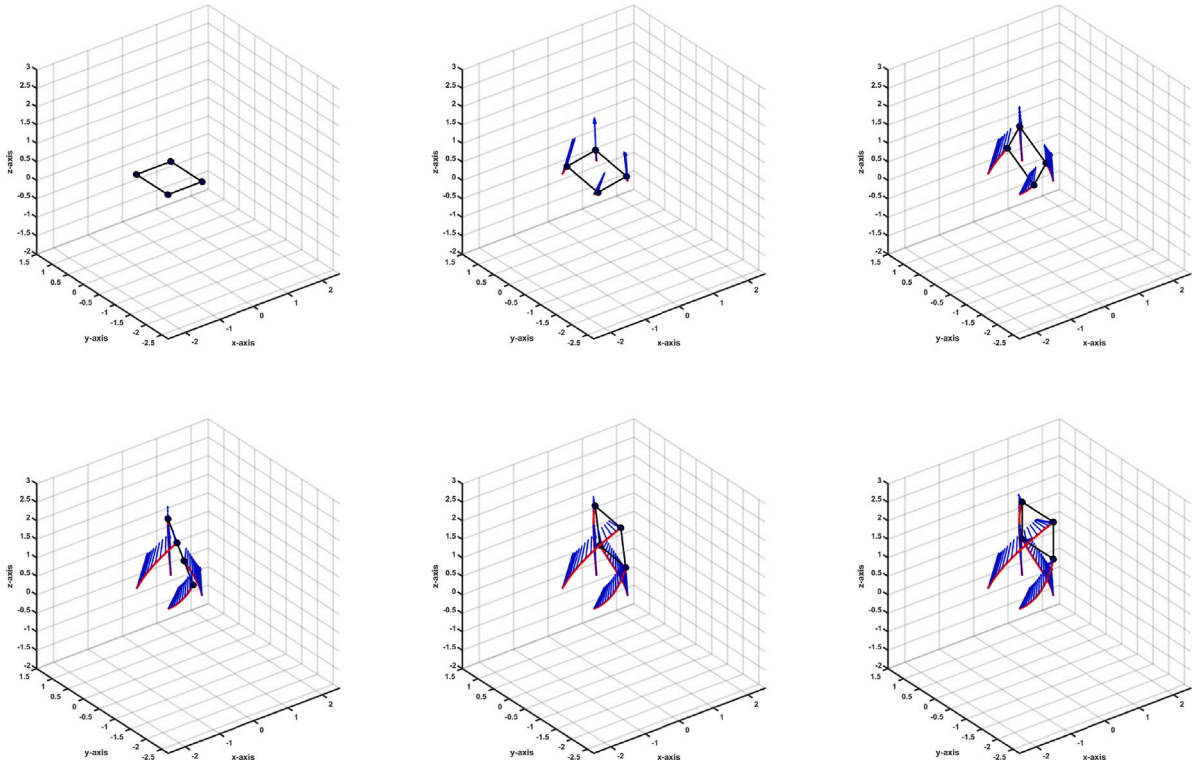


**Fig. 18.** Four linked masses: snapshots of the optimal motion at $t \in \{0,\ 0.2,\ 0.4,\ 0.6,\ 0.8,\ 1\}$. The trajectory of the mass points is shown with red lines, while the control vectors $\mathbf{u}_k$ are indicated with blue arrows.

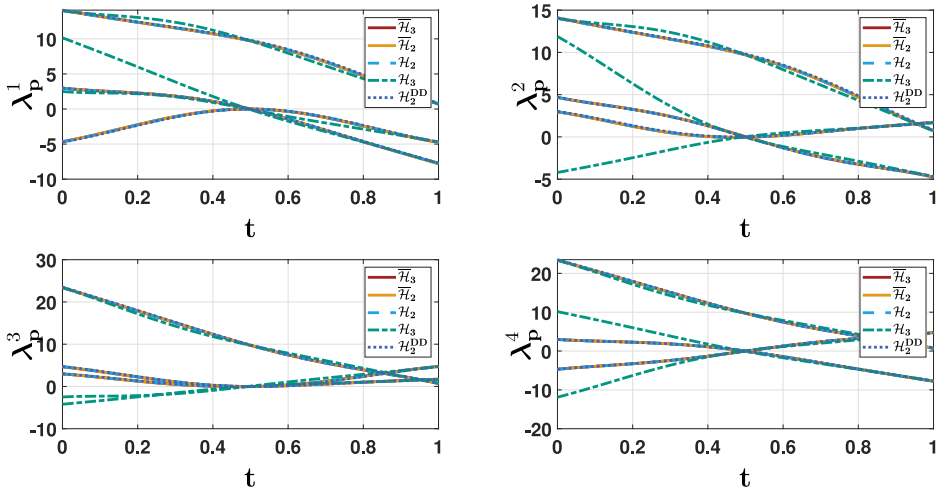


**Fig. 19.** Evolution of the adjoint variables $\lambda_{\mathbf{p}}^k$ over time. In order to identify the solutions of $\lambda_{\mathbf{p}}^k(t)$, the final values of the various results are about $\lambda_{\mathbf{p}}^1(t_f) = (-8,-5,1)^T$, $\lambda_{\mathbf{p}}^2(t_f) = (2,-5,1)^T$, $\lambda_{\mathbf{p}}^3(t_f) = (2,5,1)^T$ and $\lambda_{\mathbf{p}}^4(t_f) = (-8,5,1)^T$.

As expected (cf. Section 6.2.1), all of the schemes at hand conserve the 3-component of the generalized angular momentum $\mathbf{J}$ up to numerical round-off (Figs. 21 and 22). The numerical results reveal that also $J_1 = \mathbf{e}_1^T\mathbf{J}$ is a conserved quantity. Note that this is not a general result but due to the specific data chosen for this example. Similarly, as has been shown in Section 6.2.1, the three components of the generalized linear momentum (118) are conserved (Figs. 23 and 24).

Eventually, the convergence behavior of the schemes at hand is shown in Fig. 25. Similarly to the last example, the reference solution was calculated with scheme $\mathcal{H}_2^{\mathrm{DD}}$ and $N = 20\,000$ time intervals. The results shown in Fig. 25 confirm those obtained for the last example (cf. Fig. 11).

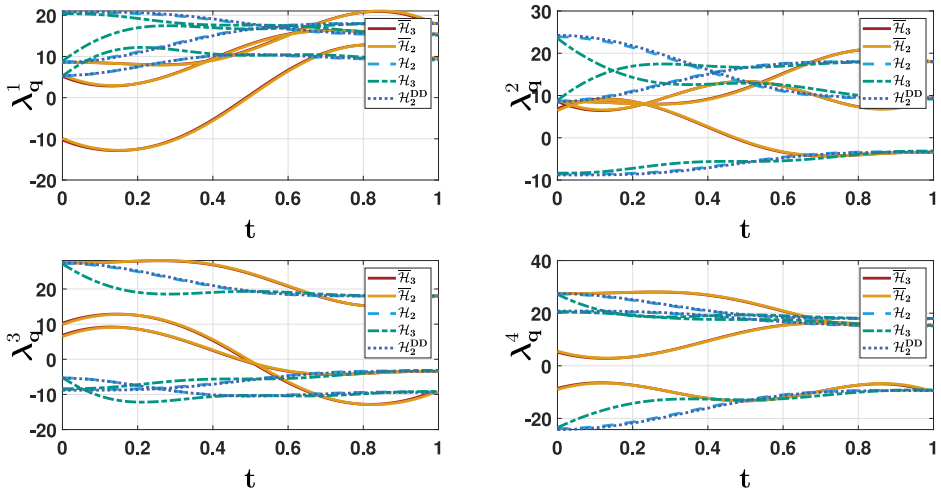


**Fig. 20.** Evolution of the adjoint variables $\lambda_{\mathbf{q}}^k$ over time. In order to identify the solutions of $\lambda_{\mathbf{q}}^k(t)$, the final values of the various results are about $\lambda_{\mathbf{q}}^1(t_f) = (15, 9, 18)^T$, $\lambda_{\mathbf{q}}^2(t_f) = (-3, -9, 18)^T$, $\lambda_{\mathbf{q}}^3(t_f) = (-3, 9, 18)^T$ and $\lambda_{\mathbf{q}}^4(t_f) = (15, -9, 18)^T$.

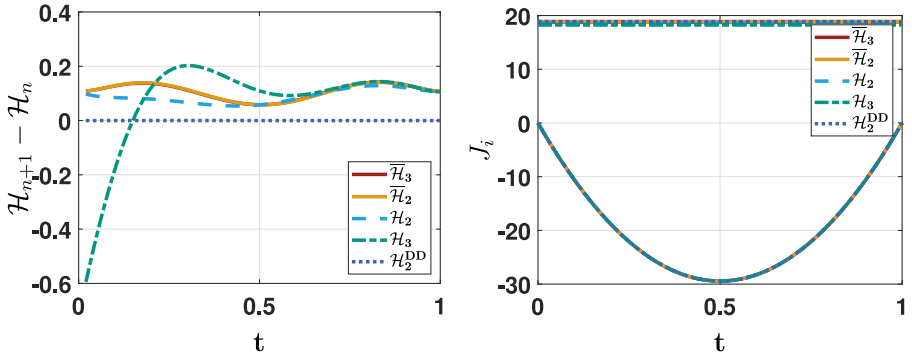


**Fig. 21.** Evolution of the optimal control Hamiltonian over time (left), and components $J_i$ of the generalized angular momentum (117) (right).

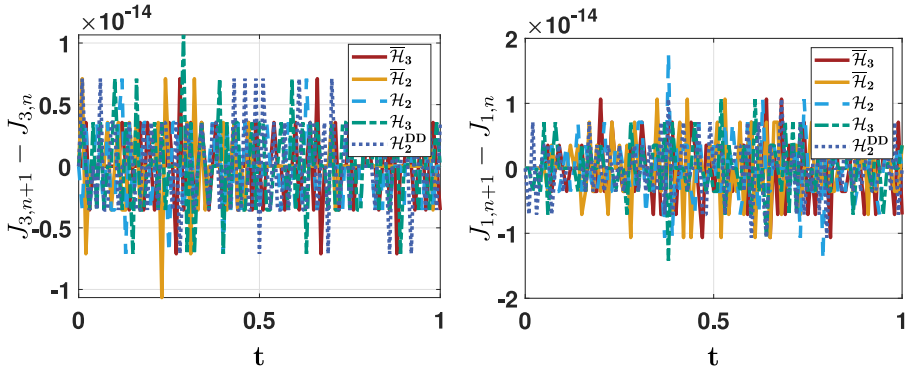


**Fig. 22.** Incremental change of the conserved generalized angular momenta $J_3$ and $J_1$.

## 7. Reconciliation of the two alternative optimal control formulations

Our numerical results provide strong evidence that the two alternative approaches to the formulation of the optimal control problem are essentially equivalent. In particular, the numerical results for the control inputs and the state variables turn out to be practically indistinguishable. On the other hand, while the results for the mechanical quantities coincide, the adjoint variables often

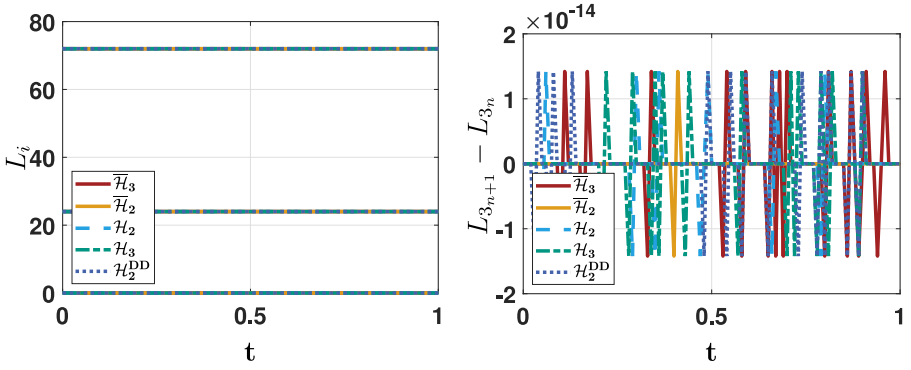


**Fig. 23.** Components $L_i$ of the generalized linear momentum (118) and incremental change of $L_3$.

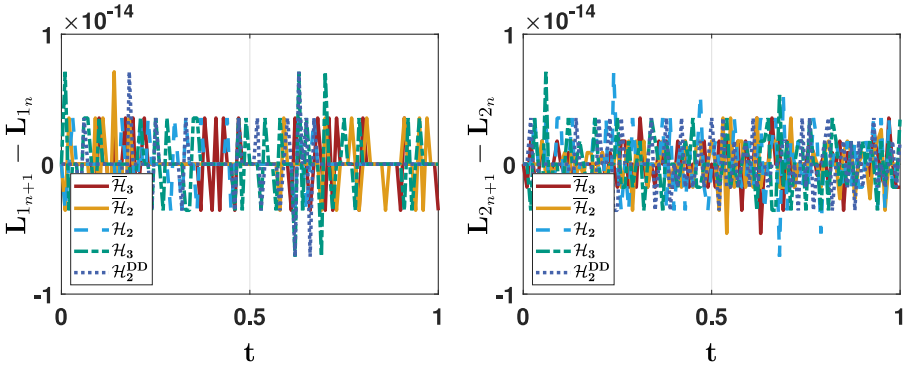


**Fig. 24.** Incremental change of components $L_1$ and $L_2$ of the generalized linear momentum (118).

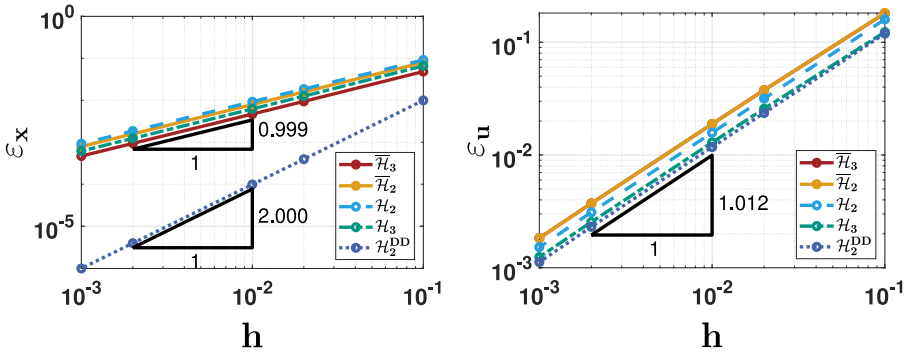


**Fig. 25.** Convergence behavior of the alternative schemes.

differ quite markedly. In this section we further elaborate on the link between the two alternative formulations. Due to numerical evidence we assume that the mechanical quantities $(\mathbf{x}, \mathbf{y}_i, \mathbf{u})$ coincide in the sequel.

### 7.1. Stabilized index-2 state DAEs

Taking into account definition (28) of the constraints $\widetilde{\mathbf{g}}_2$ implies that $\widetilde{\mathbf{g}}_2 = \frac{d}{dt}\mathbf{g}_2(\mathbf{x})$. Thus, we get the relation

$$\boldsymbol{\eta}_2^T \widetilde{\mathbf{g}}_2 = \frac{d}{dt}\left(\boldsymbol{\eta}_2^T \mathbf{g}_2(\mathbf{x})\right) - \dot{\boldsymbol{\eta}}_2^T \mathbf{g}_2(\mathbf{x})$$

Making use of the last equation, we may write

$$\mathcal{S}_2[\mathbf{x}, \mathbf{y}_2, \mathbf{u}, \lambda, \boldsymbol{\eta}_2] + \left[\boldsymbol{\eta}_2^T \mathbf{g}_2(\mathbf{x})\right]_{t_0}^{t_f} = \overline{\mathcal{S}}_2[\mathbf{x}, \mathbf{y}_2, \mathbf{u}, \overline{\lambda}, \overline{\boldsymbol{\eta}}_2] \tag{119}$$

where $\overline{\boldsymbol{\eta}}_2 = -\dot{\boldsymbol{\eta}}_2$, and the augmented cost functionals $\mathcal{S}_2$ and $\overline{\mathcal{S}}_2$ have been introduced in (33) and (34), respectively. Note that, since the constraints are satisfied at the end-points, i.e. $\mathbf{g}_2(\mathbf{x}_0) = \mathbf{g}_2(\mathbf{x}_f) = \mathbf{0}$, (119) implies that $\mathcal{S}_2 = \overline{\mathcal{S}}_2$. Relation (119) complies with the equality

$$\lambda^T \dot{\mathbf{x}} - \mathcal{H}_2(\mathbf{x}, \mathbf{y}_2, \mathbf{u}, \lambda, \boldsymbol{\eta}_2) + \frac{d}{dt}\left(\boldsymbol{\eta}_2^T \mathbf{g}_2(\mathbf{x})\right) = \overline{\lambda}^T \dot{\mathbf{x}} - \overline{\mathcal{H}}_2(\mathbf{x}, \mathbf{y}_2, \mathbf{u}, \overline{\lambda}, \overline{\boldsymbol{\eta}}_2)$$

or

$$\dot{\mathbf{x}}^T \left(\lambda - \overline{\lambda} + D\mathbf{g}_2(\mathbf{x})^T \boldsymbol{\eta}_2\right) + \dot{\boldsymbol{\eta}}_2^T \mathbf{g}_2(\mathbf{x}) - \left(\mathcal{H}_2 - \overline{\mathcal{H}}_2\right) = \mathbf{0}$$

Since the last equation is required to hold for all choices of $\dot{\mathbf{x}}$ and $\dot{\boldsymbol{\eta}}_2$, we obtain

$$\overline{\lambda} = \lambda + D\mathbf{g}_2(\mathbf{x})^T \boldsymbol{\eta}_2 \tag{120}$$

together with $\mathbf{g}_2(\mathbf{x}) = \mathbf{0}$ and $\mathcal{H}_2 = \overline{\mathcal{H}}_2$. Accordingly, the transformation of the adjoint system is governed by (120) and $\overline{\boldsymbol{\eta}}_2 = -\dot{\boldsymbol{\eta}}_2$. The transformation formulas for the adjoint variables can be written in the more detailed form

$$\overline{\lambda}_{\mathbf{q}} = \lambda_{\mathbf{q}} + D\mathbf{g}^{q^T} \boldsymbol{\eta}_2^v + \partial_{\mathbf{q}} \mathbf{g}^{v^T} \boldsymbol{\eta}_2^a \tag{121a}$$

$$\overline{\lambda}_{\mathbf{p}} = \lambda_{\mathbf{p}} + \partial_{\mathbf{p}} \mathbf{g}^{v^T} \boldsymbol{\eta}_2^a \tag{121b}$$

together with

$$\overline{\boldsymbol{\eta}}_2^q = -\dot{\boldsymbol{\eta}}_2^v \tag{122a}$$

$$\overline{\boldsymbol{\eta}}_2^v = -\dot{\boldsymbol{\eta}}_2^a \tag{122b}$$

### 7.1.1. Mathematical pendulum

The transformation formulas (121) and (122) can be easily applied to the example of the pendulum dealt with in Section 6.1. Accordingly, substitution from (110) into (121) yields

$$\overline{\lambda}_{2_{\mathbf{q}}} = \left(\mathbf{I} - \frac{1}{l_0^2}\mathbf{q}\mathbf{q}^T\right)\lambda_{2_{\mathbf{q}}} + \frac{1}{l_0^2}\left(\mathbf{q}\mathbf{p}^T - \mathbf{p}\mathbf{q}^T\right)\lambda_{2_{\mathbf{p}}} \tag{123a}$$

$$\overline{\lambda}_{2_{\mathbf{p}}} = \left(\mathbf{I} - \frac{1}{l_0^2}\mathbf{q}\mathbf{q}^T\right)\lambda_{2_{\mathbf{p}}} \tag{123b}$$

These formulas can be used to transform the results for $(\lambda_{2_{\mathbf{q}}}, \lambda_{2_{\mathbf{p}}})$ to those for $(\overline{\lambda}_{2_{\mathbf{q}}}, \overline{\lambda}_{2_{\mathbf{p}}})$ (cf. Fig. 6). Because of the numerical result $\eta_2^a = 0$ (see Fig. 8), formula (110b) implies that $\mathbf{q}^T \lambda_{2_{\mathbf{p}}} = 0$. Accordingly, $\lambda_{2_{\mathbf{p}}}$ lies already in the tangent plane $\mathcal{T}_q\mathcal{Q}$, so that transformation formula (123b) yields $\overline{\lambda}_{2_{\mathbf{p}}} = \lambda_{2_{\mathbf{p}}}$, which is in line with the results shown in Fig. 6. Moreover, the validity of (122) can be easily checked by employing (100) and (110). In particular, the numerical result $\eta_2^a = 0$ (see Fig. 8) implies that $\dot{\eta}_2^a = 0$, so that (122b) yields $\overline{\eta}_2^v = 0$, which coincides the numerical result depicted in Fig. 8.

## 7.2. Index-3 state DAEs

Definition (27) of $\widetilde{\mathbf{g}}_3$ implies that $\widetilde{\mathbf{g}}_3 = \frac{d}{dt}\mathbf{g}^v(\mathbf{x}) = \frac{d^2}{dt^2}\mathbf{g}^q(\mathbf{q})$. Therefore, the relationship

$$\boldsymbol{\eta}_3^T \widetilde{\mathbf{g}}_3 = \frac{d}{dt}\left(\boldsymbol{\eta}_3^T \mathbf{g}^v(\mathbf{x})\right) - \frac{d}{dt}\left(\dot{\boldsymbol{\eta}}_3^T \mathbf{g}^q(\mathbf{q})\right) + \ddot{\boldsymbol{\eta}}_3^T \mathbf{g}^q(\mathbf{q})$$

holds. Making use of the last equation, we may write

$$\mathcal{S}_3[\mathbf{x}, \mathbf{y}_3, \mathbf{u}, \lambda, \boldsymbol{\eta}_3] + \left[\boldsymbol{\eta}_3^T \mathbf{g}^v(\mathbf{x}) - \dot{\boldsymbol{\eta}}_3^T \mathbf{g}^q(\mathbf{q})\right]_{t_0}^{t_f} = \overline{\mathcal{S}}_3[\mathbf{x}, \mathbf{y}_3, \mathbf{u}, \overline{\lambda}, \overline{\boldsymbol{\eta}}_3] \tag{124}$$

where $\overline{\boldsymbol{\eta}}_3 = \ddot{\boldsymbol{\eta}}_3$, and the augmented cost functionals $\mathcal{S}_3$ and $\overline{\mathcal{S}}_3$ have been introduced in (33) and (34), respectively. Note that, since the constraints are satisfied at the end-points, i.e. $\mathbf{g}^q(\mathbf{q}_0) = \mathbf{g}^q(\mathbf{q}_f) = \mathbf{0}$, and $\mathbf{g}^v(\mathbf{x}_0) = \mathbf{g}^v(\mathbf{x}_f) = \mathbf{0}$, (124) implies that $\mathcal{S}_3 = \overline{\mathcal{S}}_3$. Relation (124) complies with the equality

$$\lambda^T \dot{\mathbf{x}} - \mathcal{H}_3(\mathbf{x}, \mathbf{y}_3, \mathbf{u}, \lambda, \boldsymbol{\eta}_3) + \frac{d}{dt}\left(\boldsymbol{\eta}_3^T \mathbf{g}^v(\mathbf{x}) - \dot{\boldsymbol{\eta}}_3^T \mathbf{g}^q(\mathbf{q})\right) = \overline{\lambda}^T \dot{\mathbf{x}} - \overline{\mathcal{H}}_3(\mathbf{x}, \mathbf{y}_3, \mathbf{u}, \overline{\lambda}, \overline{\boldsymbol{\eta}}_3)$$

or

$$\dot{\mathbf{x}}^T \left(\lambda - \overline{\lambda} + D\mathbf{g}^v(\mathbf{x})^T \boldsymbol{\eta}_3\right) + \ddot{\boldsymbol{\eta}}_3^T \mathbf{g}^q - \left(\mathcal{H}_3 - \overline{\mathcal{H}}_3\right) = \mathbf{0}$$

Since the last equation is required to hold for all choices of $\dot{\mathbf{x}}$ and $\ddot{\boldsymbol{\eta}}_3$, we obtain

$$\overline{\lambda} = \lambda + D\mathbf{g}^v(\mathbf{x})^T \boldsymbol{\eta}_3 \tag{125}$$

together with $\mathbf{g}^q = \mathbf{0}$ and $\mathcal{H}_3 = \overline{\mathcal{H}}_3$. Accordingly, the transformation of the adjoint system is governed by (125) and $\overline{\boldsymbol{\eta}}_3 = \ddot{\boldsymbol{\eta}}_3$. The transformation formula (125) can be written in more detail as

$$\overline{\lambda}_{\mathbf{q}} = \lambda_{\mathbf{q}} + \partial_{\mathbf{q}} \mathbf{g}^{v^T} \boldsymbol{\eta}_3 \tag{126a}$$

$$\overline{\lambda}_{\mathbf{p}} = \lambda_{\mathbf{p}} + \partial_{\mathbf{p}} \mathbf{g}^{v^T} \boldsymbol{\eta}_3 \tag{126b}$$

together with $\overline{\boldsymbol{\eta}}_3 = \ddot{\boldsymbol{\eta}}_3$.

#### 7.2.1. Mathematical pendulum

The transformation of the adjoint system can again be illustrated with the example of the pendulum dealt with in Section 6.1. Accordingly, inserting (104) into (126) yields

$$\overline{\lambda}_{3_{\mathbf{q}}} = \lambda_{3_{\mathbf{q}}} - \frac{1}{l_0^2} \mathbf{p}\mathbf{q}^T \lambda_{3_{\mathbf{p}}} \tag{127a}$$

$$\overline{\lambda}_{3_{\mathbf{p}}} = \left( \mathbf{I} - \frac{1}{l_0^2} \mathbf{q}\mathbf{q}^T \right) \lambda_{3_{\mathbf{p}}} \tag{127b}$$

These formulas can be used to transform the results for $(\lambda_{3_{\mathbf{q}}}, \lambda_{3_{\mathbf{p}}})$ to those for $(\overline{\lambda}_{3_{\mathbf{q}}}, \overline{\lambda}_{3_{\mathbf{p}}})$ (cf. Fig. 7).

## 8. Conclusion

We have made a comparison of two alternative avenues to the formulation of the optimal control of constrained mechanical systems, whose motion is governed by either index-3 or stabilized index-2 DAEs. In addition to that, we have developed structure-preserving numerical methods which are capable to preserve generalized momentum maps associated with symmetries of the underlying optimal control problem. Of paramount importance for mechanical systems are rotational symmetries which lead to the conservation of generalized angular momentum maps. These generalized angular momentum maps are quadratic invariants of the optimal control problem. Our newly devised direct discretization approach (i) yields conservation of the aforementioned quadratic invariants, and (ii) is equivalent to the indirect discretization approach.

The main difference between the two alternative formulations of the optimal control problem lies in the way, in which the holonomic constraints enter the optimal control Hamiltonian. While the common approach makes direct use of the constraints, the maximum principle relies on the acceleration level constraints if the state DAEs have index 3, and both acceleration and velocity level constraints if the state DAEs have index 2. This difference essentially affects the form of the adjoint system and the optimality condition. In particular, we have seen that the adjoint equations associated with the maximum principle form DAEs of index 1 for the adjoint variables, independent of the index of the underlying state DAEs ($i = 3$ or $i = 2$). In contrast to that, the common approach yields adjoint equations which form DAEs whose index for the adjoint variables is equal to that of the underlying state DAEs.

Our numerical investigations have shown that the two alternative optimal control formulations at hand yield optimal trajectories which are practically equivalent to each other. We further uncovered transformation formulas for the adjoint variables of the two alternative formulations (Section 7).

The newly devised direct discretization approach can be applied in a straightforward way when using the common approach. In essence, the proposed method is limited to first order accuracy since the fulfillment of the constraints requires $\alpha = 1$. Despite the structural discrepancy of the maximum principle (Remark 1) it is possible to apply the direct discretization approach in accord with the maximum principle (Section 5.2.2). This method, however, is confined to stabilized index-2 state DAEs ($i = 2$) and first-order accuracy ($\alpha = 1$). In addition to that, we newly proposed (Section 5.2.3) an alternative procedure to overcome the structural discrepancy, and which also conforms with the maximum principle. This method is based on the use of the notion of "discrete derivative" and is again confined to stabilized index-2 state DAEs ($i = 2$) but facilitates second-order accuracy ($\alpha = \frac{1}{2}$). The improved accuracy of this scheme (labeled $\mathcal{H}_2^{\mathrm{DD}}$) also results in a significantly improved approximation of the optimal control Hamiltonian, which is another conserved quantity of the optimal control problem[1].

The development of higher-order schemes would be a worthwhile goal for future work. While the focus of the present work lies on minimal control effort problems, the inclusion of alternative cost functions would also be of interest. In particular, the explicit presence of the constraint forces in the state DAEs facilitates their inclusion in the cost function. Although the use of redundant coordinates often yields constant mass matrices, the extension of our work to non-constant mass matrices should be a straightforward exercise. Similarly, the inclusion of dissipative phenomena and rheonomic constraints would be worth further investigation. In particular, it should be clarified how these additional features affect the symmetry of the optimal control problem.

## CRediT authorship contribution statement

**Simeon Schneider:** Writing – review & editing, Writing – original draft, Visualization, Validation, Software, Methodology, Investigation, Formal analysis, Conceptualization. **Peter Betsch:** Writing – review & editing, Writing – original draft, Supervision, Resources, Project administration, Methodology, Investigation, Funding acquisition, Formal analysis, Conceptualization.

[1] Algorithmic conservation of the optimal control Hamiltonian has been achieved recently [33] in the context of optimal control of ODEs.

## Declaration of competing interest

The authors declare the following financial interests/personal relationships which may be considered as potential competing interests: Peter Betsch reports financial support was provided by German Research Foundation. If there are other authors, they declare that they have no known competing financial interests or personal relationships that could have appeared to influence the work reported in this paper.

## Data availability

Data will be made available on request.

## Acknowledgments

This work has been supported financially by the Deutsche Forschungsgemeinschaft (DFG, German Research Foundation), Germany – Projektnummer 442997215.

## References

[1] R. Bordalba, T. Schoels, L. Ros, J. Porta, M. Diehl, Direct collocation methods for trajectory optimization in constrained robotic systems, IEEE Trans. Robot. 39 (1) (2023) 183–202, http://dx.doi.org/10.1109/TRO.2022.3193776.
[2] P. Kunkel, V. Mehrmann, Differential-Algebraic Equations. Analysis and Numerical Solution, European Mathematical Society Publishing House, Zurich, 2006.
[3] B. Simeon, Computational flexible multibody dynamics. A differential-algebraic approach, in: Differential-Algebraic Equations Forum, Springer-Verlag, 2013.
[4] M. Gerdts, Optimal Control of ODEs and DAEs, second ed., De Gruyter Oldenbourg, Berlin/Boston, 2024, http://dx.doi.org/10.1515/9783110797893.
[5] C. Gear, G. Gupta, B. Leimkuhler, Automatic integration of the Euler-Lagrange equations with constraints, J. Comput. Appl. Math. 12&13 (1985) 77–90.
[6] J. Betts, Practical Methods for Optimal Control and Estimation Using Nonlinear Programming, second ed., SIAM, Philadelphia, PA, 2010.
[7] S. Ober-Blöbaum, O. Junge, J. Marsden, Discrete mechanics and optimal control: An analysis, ESAIM Control Optim. Calc. Var. 17 (2) (2011) 322–352.
[8] S. Leyendecker, S. Ober-Blöbaum, J. Marsden, M. Ortiz, Discrete mechanics and optimal control for constrained systems, Optim. Control Appl. Methods 31 (6) (2010) 505–528.
[9] P. Betsch, R. Siebert, N. Sänger, Natural coordinates in the optimal control of multibody systems, J. Comput. Nonlinear Dynam. 7 (1) (2012) 011009/1–8, http://dx.doi.org/10.1115/1.4004886.
[10] M. Schubert, R. Sato Martín de Almagro, K. Nachbagauer, S. Ober-Blöbaum, S. Leyendecker, Discrete adjoint method for variational integration of constrained ODEs and its application to optimal control of geometrically exact beam dynamics, Multibody Syst. Dyn. 60 (3) (2024) 447–474, http://dx.doi.org/10.1007/s11044-023-09934-4.
[11] E. Pinch, Optimal Control and the Calculus of Variations, Oxford University Press, 1993, http://dx.doi.org/10.1093/oso/9780198532170.003.0001.
[12] T. Roubíček, M. Valášek, Optimal control of causal differential–algebraic systems, J. Math. Anal. Appl. 269 (2) (2002) 616–641.
[13] C. Bottasso, A. Croce, Optimal control of multibody systems using an energy preserving direct transcription method, Multibody Syst. Dyn. 12 (1) (2004) 17–45.
[14] W. Steiner, S. Reichl, The optimal control approach to dynamical inverse problems, J. Dyn. Sys., Meas., Control 134 (2) (2012) 021010/1–13.
[15] G. Bastos, R. Seifried, O. Brüls, Inverse dynamics of serial and parallel underactuated multibody systems using a DAE optimal control approach, Multibody Syst. Dyn. 30 (3) (2013) 359–376.
[16] Y. Cao, S. Li, L. Petzold, R. Serban, Adjoint sensitivity analysis for differential-algebraic equations: The adjoint DAE system and its numerical solution, SIAM J. Sci. Comput. 24 (3) (2003) 1076–1089, http://dx.doi.org/10.1137/S1064827501380630.
[17] K. Nachbagauer, S. Oberpeilsteiner, K. Sherif, W. Steiner, The use of the adjoint method for solving typical optimization problems in multibody dynamics, J. Comput. Nonlinear Dynam. 10 (2015) 061011/1–10.
[18] A. Bijalwan, S. Schneider, P. Betsch, J. Muñoz, Monolithic and staggered solution strategies for constrained mechanical systems in optimal control problems, 2024, Submitted for publication.
[19] M. Gerdts, Local minimum principle for optimal control problems subject to differential-algebraic equations of index two, J. Optim. Theory Appl. 130 (3) (2006) 441–460.
[20] B. Martens, M. Gerdts, Convergence analysis for approximations of optimal control problems subject to higher index differential-algebraic equations and mixed control-state constraints, SIAM J. Control Optim. 58 (1) (2020) 1–33.
[21] J. Sanz-Serna, Symplectic Runge-Kutta schemes for adjoint equations, automatic differentiation, optimal control, and more, SIAM Rev. 58 (1) (2016) 3–33, http://dx.doi.org/10.1137/151002769.
[22] W. Hager, Runge-Kutta methods in optimal control and the transformed adjoint system, Numer. Math. 87 (2) (2000) 247–282.
[23] J. Bonnans, J. Laurent-Varin, Computation of order conditions for symplectic partitioned Runge-Kutta schemes with application to optimal control, Numer. Math. 103 (1) (2006) 1–10.
[24] K. Flaßkamp, T. Murphey, Structure-preserving local optimal control of mechanical systems, Optim. Control Appl. Methods 40 (2) (2019) 310–329.
[25] D. Djukić, Noether's theorem for optimum control systems, Internat. J. Control 18 (3) (1973) 667–672.
[26] D. Torres, On the Noether theorem for optimal control, Eur. J. Control 8 (1) (2002) 56–63.
[27] P. Betsch, C. Becker, Conservation of generalized momentum maps in mechanical optimal control problems with symmetry, Internat. J. Numer. Methods Engrg. 111 (2) (2017) 144–175, http://dx.doi.org/10.1002/nme.5459.
[28] P. Betsch, S. Schneider, Conservation of generalized momentum maps in the optimal control of constrained mechanical systems, IFAC PapersOnLine 54 (9) (2021) 615–619, http://dx.doi.org/10.1016/j.ifacol.2021.06.123.
[29] P. Kinon, P. Betsch, S. Schneider, The GGL variational principle for constrained mechanical systems, Multibody Syst. Dyn. 57 (3–4) (2023) 211–236, http://dx.doi.org/10.1007/s11044-023-09889-6.
[30] P. Kinon, P. Betsch, S. Schneider, Structure-preserving integrators based on a new variational principle for constrained mechanical systems, Nonlinear Dynam. 111 (2023) 14231–14261, http://dx.doi.org/10.1007/s11071-023-08522-7.
[31] O. Gonzalez, Time integration and discrete Hamiltonian systems, J. Nonlinear Sci. 6 (1996) 449–467.
[32] S. Schneider, P. Betsch, On optimal control problems in redundant coordinates, in: Proceedings of the ECCOMAS Thematic Conference on Multibody Dynamics, Lisbon, Portugal, 2023, pp. 1–10.
[33] A. Bijalwan, J. Muñoz, A control Hamiltonian-preserving discretisation for optimal control, Multibody Syst. Dyn. 59 (1) (2023) 19–43, http://dx.doi.org/10.1007/s11044-023-09902-y.